Am J Cancer Res 2024;14(8):3733-3756
www.ajcr.us /ISSN:2156-6976/ajcr0158384

Original Article

PPIH as a poor prognostic factor increases cell proliferation and m6A RNA methylation in hepatocellular carcinoma

Xiao-Xia Chi[1,2*], Peng Ye[3*], Neng-Qi Cao[4*], Wei-Lun Hwang[5], Jong-Ho Cha[6], Mien-Chie Hung[7], Kai-Wen Hsu[8], Xiu-Wen Yan[1], Wen-Hao Yang[9]

[1]Affiliated Cancer Hospital and Institute, Guangzhou Medical University, Guangzhou 510095, Guangdong, China; [2]Department of Family Medicine, The University of Hong Kong-Shenzhen Hospital, Shenzhen 518053, Guangdong, China; [3]Infection Medicine Research Institute of Panyu District, The Affiliated Panyu Central Hospital of Guangzhou Medical University, Guangzhou 511400, Guangdong, China; [4]Department of General Surgery, Nanjing Lishui People's Hospital, Nanjing 211200, Jiangsu, China; [5]Department of Biotechnology and Laboratory Science in Medicine, and Cancer Progression Research Center, National Yang Ming Chiao Tung University, Taipei 112304, Taiwan; [6]Department of Biomedical Science and Engineering, Graduate School, Inha University, Incheon 22212, The Republic of Korea; [7]Graduate Institute of Biomedical Sciences, Institute of Biochemistry and Molecular Biology, Research Center for Cancer Biology, Cancer Biology and Precision Therapeutics Center, and Center for Molecular Medicine, China Medical University, Taichung 406040, Taiwan; [8]Institute of Translational Medicine and New Drug Development, China Medical University, Taichung 404328, Taiwan; [9]Graduate Institute of Cell Biology, and Cancer Biology and Precision Therapeutics Center, China Medical University, Taichung 404327, Taiwan. [*]Equal contributors.

Received June 10, 2024; Accepted August 7, 2024; Epub August 25, 2024; Published August 30, 2024

Abstract: RNA-binding proteins (RBPs) play a crucial role in the biological processes of liver hepatocellular carcinoma (LIHC). Peptidyl-prolyl cis-trans isomerase H (PPIH), an RBP, possesses prolyl isomerase activity and functions as a protein chaperone. The relationship between PPIH and LIHC has not yet been fully elucidated. This study elucidated potential mechanisms through which PPIH affects the prognosis of LIHC. Bioinformatics analysis and in vitro experiments revealed that PPIH expression was higher in LIHC tissues than in normal tissues. PPIH was identified as an independent prognostic factor, with high PPIH expression being associated with worse prognoses. Moreover, PPIH increased the m6A RNA methylation level and promoted cell proliferation by modulating DNA replication and the expression of cell cycle-related genes in LIHC cells. Bioinformatics analysis also revealed that PPIH expression increased immune cell infiltration and the expression of immune checkpoint proteins. Collectively, these findings indicate that PPIH might promote LIHC progression by enhancing the m6A RNA methylation level, increasing cell proliferation, and altering the tumor immune microenvironment. Our study demonstrates that PPIH, as a poor prognostic factor, may lead to LIHC malignancy through multiple pathways. Further in-depth research on this topic is warranted.

Keywords: RNA-binding protein, PPIH, hepatocellular carcinoma, m6A RNA methylation, tumor immune microenvironment, cell cycle

Introduction

Liver hepatocellular carcinoma (LIHC) is a highly prevalent and lethal type of malignant tumor that is associated with high morbidity and mortality. LIHC is a leading cause of cancer-related mortality and adversely affects patient health and quality of life [1, 2]. LIHC mainly occurs in the liver and can be classified as primary hepatocellular carcinoma, which is the most common form, and metastatic hepatocellular carcinoma [3]. The pathogenesis of LIHC is complex and influenced by various factors, including viral infection (hepatitis B virus and hepatitis C virus), chronic alcohol consumption, obesity, diabetes mellitus, and metabolic syndrome [4]. In addition, genetic and environmental factors and lifestyle habits play a crucial role in the onset of this disease [4]. The occurrence and development of LIHC is a multifactorial and

https://doi.org/10.62347/NZIJ5785

complex process that involves several molecular mechanisms [5-9]. Mutations in various key genes can lead to the inactivation of tumor suppressor genes and the activation of oncogenes, thereby promoting the proliferation and growth of tumor cells. For example, mutations in *TP53*, *CTNNB1*, and *AXIN1* genes are commonly observed in liver cancer [10-14]. Moreover, disruptions in the cell cycle caused by the abnormal expression of or mutations in cell cycle regulatory genes, such as *p21* (*Cip1/CDKN1A*), *p27* (*Kip1/CDKN1B*), *MCM4*, *CHEK1*, and *KAT2B*, can lead to the aberrant proliferation of liver cancer cells, further driving tumor development [15, 16]. The unique immune microenvironment of LIHC, characterized by immune infiltrating cells and immune factors, affects treatment outcomes and prognoses through various mechanisms [17-19]. Epigenetic alterations, such as DNA methylation and histone modification, play crucial roles in the occurrence and development of LIHC [20]. Abnormal m6A RNA methylation can lead to the aberrant expression of LIHC-promoting genes and regulate cell proliferation, metastasis, and drug resistance, thereby affecting the progression of LIHC [21-23]. Conducting in-depth research on these pathogenic factors is essential for developing new therapeutic strategies and improving survival and quality of life in patients with LIHC. Currently, the primary treatment options for liver cancer include local ablation, interventional therapy, radiotherapy, chemotherapy, targeted therapy, immunotherapy, and surgical resection [2, 24, 25]. However, these treatment options have limited efficacy in cases of advanced liver cancer [26, 27]. Thus, conducting further in-depth research on the pathogenesis of liver cancer and related detection and treatment strategies is essential. We can effectively reduce the morbidity and mortality of liver cancer by enhancing preventive measures, increasing early diagnosis rates, and improving treatment methods, and doing so will mitigate the disease's threat to human health. Increasing evidence has indicated that RNA-binding proteins (RBPs) play a crucial role in the biological processes of liver cancer, including gene expression regulation, cell signal transduction, cell proliferation, metastasis, and invasion [10, 28-33]. Thus, identification of new RBPs associated with LIHC progression and elucidation of the underlying mechanisms of LIHC could lead to new therapeutic targets for patients with LIHC.

RBPs are a type of protein that specifically bind to RNA and play key roles in RNA synthesis, processing, and metabolism [34]. In addition, RBPs are essential for the posttranscriptional regulation of genes. RBPs can recognize and specifically bind to RNA through specific RNA binding domains, forming ribonucleoprotein complexes that regulate gene expression [35]. Moreover, RBPs are involved in various stages of the mRNA lifecycle, including splicing, exportation, localization, stability, and translation [36]. RBPs can bind to RNA in the cytoplasm or nucleus and perform different functions in each location. In the cytoplasm, RBPs are primarily involved in mRNA stabilization and transport, translation, stress response, mitochondrial function, and autophagy regulation [37]. By contrast, in the nucleus, RBPs are mainly involved in RNA maturation processes [38]. RBPs frequently shuttle between the cytoplasm and nucleus and other cytoplasmic compartments, such as stress granules and P-bodies [39]. RBPs play crucial roles in various tumors, including liver cancer [40], acute myeloid leukemia [41], breast cancer [42], colorectal cancer [43], and lung cancer [44]. In addition, RBPs regulate various aspects of tumor biology, including the extracellular matrix [45], extracellular matrix-receptor interactions [46], cell adhesion [47], cell polarity and epithelial-mesenchymal transition [48], cell proliferation and migration [49-51], and cell cycle progression [52]. The aforementioned mechanisms indicate the crucial role of RBPs in tumorigenesis and tumor progression and prognosis. Although numerous RBPs associated with liver cancer have been widely studied, most of them have been used primarily for diagnostic and prognostic purposes. Currently, RBPs that can serve as effective targets for cancer treatment are lacking. Moreover, the development of therapeutic RBPs remains limited. Thus, the functional significance of RBPs in the pathogenesis of LIHC should be determined to identify new therapeutic targets and biomarkers for LIHC and develop effective treatment approaches.

In this study, we analyzed RNA-seq data, survival data, and relevant clinical features from the LIHC cohort in The Cancer Genome Atlas (TCGA) public database. We performed a comparative analysis by using the RBP gene set and identified the RBP PPIH. We observed that

PPIH was highly expressed in LIHC tissues and that the expression of PPIH was strongly associated with poor prognosis in cases of LIHC. Moreover, through bioinformatics analysis and experimental validation, we confirmed that PPIH regulates the expression of genes related to m6A RNA methylation and promotes m6A methylation modification in hepatocellular carcinoma. Our findings indicate that the activity of PPIH may alter the immune microenvironment of LIHC by regulating immune cells, inflammatory factors, and other elements surrounding the tumor. In addition, PPIH promotes cell proliferation by enhancing signaling pathways involved in the cell cycle and DNA replication. In conclusion, PPIH contributes to the progression of LIHC by upregulating m6A RNA methylation, modifying the immune microenvironment, and regulating the cell cycle. Our study provides new insights into the oncogenic role of PPIH in LIHC, suggesting its potential as a new prognostic and diagnostic marker and as a target for guiding interventional therapies in patients with LIHC.

Materials and methods

Bioinformatics analysis

We obtained data on patients with LIHC from the TCGA LIHC cohort (https://tcga-data.nci.nih.gov/tcga/). We collected data on gene expression, mutations, and clinical information for 374 tumor samples and 50 adjacent normal tissue samples. We downloaded the gene-level expression data for PPIH from the TCGA-LIHC project in FPKM format from the GDC data portal (https://portal.gdc.cancer.gov/). The expression of PPIH in the TCGA-LIHC cohort was classified as high or low on the basis of the median expression value. We used the TIMER2.0 database (http://timer.comp-genomics.org/timer/) to analyze gene expression levels in TCGA. Protein-protein interactions (PPIs) were analyzed using STRING (https://www.string-db.org/) and Cytoscape 3.10.1. The Kaplan-Meier plotter was used to investigate the effect of PPIH expression on prognosis. We analyzed data from liver cancer tissues and nontumor groups across several data sets: GSE10143, GSE36376, GSE63898, and GSE54236. GSE10143 included 80 tumor samples and 307 nontumor liver tissue samples from patients with LIHC. GSE36376 included 240 hepatocellular carcinoma samples and 193 adjacent tissue samples. GSE63898 included 228 hepatocellular carcinoma samples and 168 liver cirrhosis samples, and GSE54236 included 81 tumor tissue samples and 80 adjacent nontumor tissue samples. The MCPcounter algorithm in CAMOIP (http://www.camoip.net/) was used to compare immune-infiltrating cell scores between the low and high PPIH expression groups in the TCGA-LIHC cohort. This analysis was performed to examine the relationship between PPIH expression and tumor immunity. In addition, gene set enrichment analysis (GSEA) was conducted using GSEA software (version 4.1.0, http://software.broadinstitute.org/gsea).

Cell culture

All cell lines are preserved at the Cancer Immunology Center, State Key Laboratory of Respiratory Diseases, Guangzhou Medical University. HEK293T cells and the human hepatocellular carcinoma cell lines Huh7, HepG2, and MHCC97H were cultured in Dulbecco's modified Eagle medium (06-1055-57-1ACS, BI). The human hepatocellular carcinoma cell lines Bel7402 and Li7 were cultured in RPMI 1640 medium (C11330500BT, Gibco), and PLC/PRF/5 cells were cultured in minimum essential medium (C11095500BT, Gibco). All media were supplemented with 10% inactivated fetal bovine serum (04-001-1ACS, BI) and 1% penicillin-streptomycin (15140122, Thermo Fisher Scientific, Waltham, MA, USA). The cells were maintained in a 37°C incubator under 5% carbon dioxide.

Transient transfection

HEK-293T cells were plated into six well plates approximately 24 hours prior to transfection. Cells were transfected in serum-free medium using 3 μg plasmid DNA and 9 μg Polyethylenimine hydrochloride (764965-1G, Sigma-Aldrich, USA) according to the manufacture's instructions. 6-10 hours after transfection, the culture medium was replaced with fresh DMEM medium containing 10% FBS and incubated for an additional 72 hours. Finally, cells were harvested and proteins were extracted for western blot analysis to validate knockdown efficiency by detecting target protein levels. For specific sequences of plasmid inserts, please see the Table S1.

Cell transfection

The plasmids used for constructing stable cell lines were purchased from Tsingke (Beijing, China). The plasmids containing short hairpin RNA directed against PPIH are provided in supplementary materials (Table S1). pCDH-CMV-MCS-EF1-Puro plasmid was used for expression vector. The complementary DNA (cDNA) clone of PPIH was subcloned into pCDH-CMV-MCS-EF1-Puro vector for PPIH overexpression, using the forward primer sequence 5'-TGCTCTAGAATGGCGGTGGCAAATTCAAG-3' and reverse primer sequence 5'-CGGGATCCCTACATCTCCCCACACTGCG-3'. psPAX2 and pMD2.G packaging vectors were used to produce lentiviruses. Hepatocellular carcinoma cell lines stably expressing PPIH were developed through lentiviral transfection. Polybrene (40804ES76, Yeasen, Shanghai, China) was used to enhance infection efficiency. Following transfection, the cells were selected using puromycin (ST551, Beyotime, Shanghai, China) to ensure the stable expression of PPIH. The efficiency of transfection was confirmed through quantitative polymerase chain reaction (qPCR) and Western blot (WB) analysis.

Western blot

The cells from each group were harvested and lysed using RIPA buffer (P0013B, Beyotime) supplemented with a protease inhibitor cocktail (P1005, Beyotime). The mixture was placed on ice for 30 minutes. The total protein was then extracted through centrifugation at 4°C, and its concentration was measured using a BCA kit (23227, Thermo Fisher). Proteins were mixed with 5 × loading buffer (CW0027S, Jiangsu, China) in a ratio of 4:1, denatured at 95°C for 10 minutes, and then loaded onto a sodium dodecyl sulfate-polyacrylamide gel electrophoresis gel for electrophoresis under appropriate conditions. After electrophoresis, the proteins were transferred to a polyvinylidene difluoride membrane, which was subsequently blocked with 5% skim milk at room temperature for 1 hour. The membrane was incubated with primary antibodies at 4°C overnight, washed 3 times with TBST buffer, then incubated with a secondary antibody for 2 hours at room temperature, and washed again three times with TBST buffer. The luminol reagent (sc-2048, Santa Cruz Biotechnology, Inc. Dallas, TX, USA) was applied to the strip, and protein bands were visualized using the Tanon 5200 imaging system (Tanon, Shanghai, China). The following antibodies were used: GAPDH (1:1000, 2118S, Abcam, UK), PPIH (1:1000, ab151246, Abcam), PPIH (1:1000, GTX118224, Genetex, USA), and horseradish peroxidase-conjugated goat antirabbit secondary antibody (1:3000, 7074S, Cell Signaling Technology, USA).

Quantitative polymerase chain reaction (qPCR)

Total RNA was extracted from the cells by using a Total RNA Isolation Reagent Kit (RC101-01, Vazyme, Nanjing, China) in accordance with the manufacturer's instructions. Total RNA was then converted into cDNA by using a RevertAid PreMix Kit (M1631, Thermo Fisher Scientific Inc.). Real-time qPCR was performed using TB Green Premix Ex Taq II (Cat. RR820A, TaKaRa, Japan) on a LightCycler 480 II system (Roche, Basel, Switzerland). The qPCR results were analyzed using the $2^{-\Delta\Delta CT}$ method and presented as fold changes in gene expression. Detailed information on all gene primers used in this study are available in the supplementary materials (Table S2).

Dot blot

Dot blot analysis was performed as described previously [53]. mRNA was isolated and purified from cells by using a BeyoMa mRNA Extraction Kit (R0073S, Beyotime) and diluted to a concentration of 100 ng/μL. The mRNA samples were heated at 95°C for 5 minutes and then cooled on ice. Subsequently, 2.5 μL of each mRNA sample was directly spotted onto Hybond-N+ membranes, which were left to dry completely. The mRNA was cross-linked to the membrane by using a SCIENTZ 03-II ultraviolet crosslinker (Scientz Biotechnology, Ningbo, China) at a wavelength of 254 nm under 5 minutes of irradiation. The membrane was then blocked with 5% skim milk at room temperature for 1 hour. Then, the membrane was incubated overnight at 4°C with an anti-m6A antibody (1:1000, 68055-1-Ig, Proteintech, Wuhan, China) and washed 3 times with TBST buffer. The membrane was then incubated with a secondary antibody for 2 hours at room temperature and washed 3 more times with TBST buffer. The membrane was conjugated to a luminescent substrate and exposed.

After exposure, the membrane was stained with 0.2% methylene blue staining buffer (G1301, Beijing Solarbio Science & Technology, Beijing, China) for 30 minutes and then washed with deionized water until the background was clear before being photographed.

Immunofluorescence

The cells in the logarithmic growth phase were harvested, seeded in confocal culture dishes, and cultured for 48 hours. The cells were then fixed with 4% paraformaldehyde for 15 minutes at room temperature and washed 3 times with phosphate-buffered saline (PBS). Next, the cells were incubated in PBS buffer containing 0.1% to 0.25% Triton X-100 for 15 to 30 minutes and washed 3 times. The cells were blocked with 5% bovine serum albumin (BSA) for 1 hour, incubated overnight with an m6A antibody (1:200, 202 003, Synaptic System, Germany) at 4°C, and washed 3 times. The cells were then incubated with Alexa Fluor 568 (1:1000, A10042, Invitrogen) for 1 hour at room temperature and washed 3 more times. Cell nuclei were stained with 4',6-diamidino-2-phenylindole (DAPI) dye (P0131, Beyotime), and immunofluorescence staining images were captured using a Zeiss LSM 880 laser confocal microscope (Carl Zeiss Microscopy, Germany).

Growth curve determination

Cell growth curves were determined using a cell counting kit-8 (CCK-8, C0039, Beyotime). The cells were seeded into 96-well plates at a density of 2000 cells per well and cultured until adherence was achieved. To measure cell viability, 10 μL of CCK-8 reagent was added to every 100 μL of culture medium, and the plates were incubated for a designated period in the dark. Finally, the absorbance of each well was measured at 450 nm by using a microplate reader (Varioskan LUX, Thermo Fisher).

Plate colony formation assay

The cells in the logarithmic growth phase were harvested, and a single-cell suspension was prepared and seeded into a 6-well plate at a density of 1000 cells/well. The cells were cultured for 14 days, and the media were changed as necessary depending on cell conditions. Then, the cells were fixed with 4% paraformaldehyde for 15 minutes, stained with crystal violet dye for 30 minutes, and washed. Photographs of the wells were taken, and the number of colonies was counted. The clone formation rate was calculated using the following formula: (number of colonies/number of inoculated cells) × 100%.

Edu-555 cell proliferation assay

The cells in the logarithmic growth stage were collected and seeded in confocal culture dishes and cultured for 48 hours. The cells were incubated with Edu-labeled reagent from a BeyoClick Edu-555 Cell Proliferation Assay Kit (C0075s, Beyotime) for 2 hours (approximately 10% of the cell cycle time). The cells were then fixed with 4% paraformaldehyde and washed 3 times with PBS containing 3% BSA. The cells were then incubated in immunostaining permeabilization solution (P0096-500 ml, Beyotime) for 10 to 15 minutes and washed once or twice. The Click reaction mixture was prepared and applied to the cells for 30 minutes at room temperature in the dark, followed by 3 washes. Cell nuclei were stained with DAPI dye (P0131, Beyotime), and images were captured using a confocal microscope.

Flow cytometry analysis

A cell cycle assay kit (E-CK-A351, Elabscience Biotechnology, Wuhan, China) was used for cell cycle detection. Approximately 5×10^5 cells were harvested and resuspended in 0.3 mL of PBS. Next, 1.2 mL of anhydrous ethanol was added at -20°C, mixed thoroughly, and then placed overnight in a -20°C refrigerator for fixation. On the following day, ethanol was removed, and the cells were resuspended in PBS and left at room temperature for 15 minutes. After the removal of PBS, 100 μL of RNase A reagent was added, and the cells were thoroughly suspended and incubated at 37°C for 30 minutes. Subsequently, 400 μL of propidium iodide reagent (50 μg/mL) was added and thoroughly mixed, followed by incubation in the dark at 4°C for 30 minutes. The stained samples were analyzed using a BD Accuri C6 flow cytometer (BD Biosciences, San Jose, CA, USA). The collected data were further processed and analyzed using FlowJo software (version 10.8.1, BD Biosciences).

Statistical analysis

Statistical analyses were performed using GraphPad Prism 8 (GraphPad Software, San Diego, California, USA). All results are based on at least 3 independent experiments and are presented as the mean ± standard error of the mean. Differences between groups were assessed using Student's t test. A *P* value of < 0.05 was considered statistically significant. The levels of significance are indicated as follows: *P ≤ 0.05, **P ≤ 0.01, ***P ≤ 0.001, ****P ≤ 0.0001.

Results

PPIH is highly expressed in LIHC and associated with poor prognosis

First, we obtained gene expression data from 374 LIHC tumor samples and 50 normal tissue samples in TCGA. We identified 1484 genes that were upregulated in liver tumor tissues (|Log2FC| ≥ 1, q < 0.01) and 500 survival-related genes in LIHC (P < 0.001). Subsequently, we cross-referenced these gene sets with data sets containing 1542 RBPs [34], and identified 21 RBPs that were differentially expressed and associated with prognosis (**Figure 1A**). Using the online platform STRING (https://www.string-db.org/) and Cytoscape 3.10.1 software, we conducted a PPI analysis on these 21 RBPs. Genes that exhibited high connectivity and importance within the network may play critical regulatory roles. We used the CytoHubba plugin in Cytoscape to identify hub genes within the PPI network. The genes were scored and ranked using the density of maximum neighborhood component algorithm, a local-based method (**Figure 1B**). Among the top 10 genes, PPIH ranked first, indicating that PPIH has more interactions with other genes and may play a key regulatory role in cell signaling, metabolic pathways, or other biological processes. Thus, PPIH can serve as a crucial biomarker or therapeutic target. Although PPIH was identified as a prognostic factor [54], the mechanism through which it affects LIHC prognosis remains unclear.

We used TIMER2.0 to determine the differential mRNA expression levels of PPIH between 33 types of tumors and their adjacent normal tissues in the TCGA tumor database. This analysis was conducted to validate the expression of PPIH across various cancer types. The results revealed a significantly higher expression of PPIH in multiple cancer tissues than in normal tissues, including BLCA, BRCA, CESC, CHOL, COAD, ESCA, GBM, HNSC, KIRC, KIRP, LIHC, LUAD, LUSC, PRAD, READ, STAD and UCEC. However, the expression of PPIH was downregulated in KICH and THCA (**Figure 1C**). In addition, a conjoint analysis of the TCGA + GTEx database confirmed the increased expression of PPIH in various cancers (Figure S1A). Furthermore, we investigated the prognostic value of PPIH for overall survival (OS) across various cancers in the TCGA pan-cancer analysis. We determined that high PPIH expression was associated with poor prognosis in several cancers, including ACC (hazard ratio [HR] = 3.21216, P = 0.0054), KIRC (HR = 1.64176, P = 0.0013), KIRP (HR = 1.86689, P = 0.0425), LGG (HR = 1.93376, P = 4e-04), LIHC (HR = 2.22089, P < 0.0001), MESO (HR = 1.91159, P = 0.0079), and SARC (HR = 1.88614, P = 0.002); the prognostic value of PPIH was more pronounced in LIHC than in other cancer types (Figure S1B). In addition, we examined progression-free survival (PFS; Figure S1C), disease-free survival (DFS; Figure S1D), and disease-specific survival (DSS; Figure S1E) and determined that PPIH expression increased prognostic risk in most tumors (HR > 1), particularly in LIHC. These results indicate the importance of PPIH in evaluating the prognosis of patients with liver cancer and its potential as a prognostic biomarker for LIHC.

To further validate the expression characteristics of PPIH in patients with LIHC, we investigated its expression profile in liver cancer tissues and normal tissues by using LIHC datasets (GSE10143, GSE36376, GSE63898, GSE54236) from the GEO database. The results indicated that the expression of PPIH was higher in liver cancer tissues than in normal tissues (**Figure 1D**). Furthermore, survival curve analysis performed using the Kaplan-Meier plotter database with Affymetrix microarray data revealed that higher PPIH expression was associated with poorer OS (HR = 1.54, P = 0. 014), PFS (HR = 1.44, P = 0.017), relapse-free survival (RFS; HR = 1.56, P = 0.015), and DSS (HR = 1.79, P = 0.011; **Figure 1E**), These results indicate that high PPIH expression is a significant risk factor among various prognostic indicators in LIHC. Early studies have reported

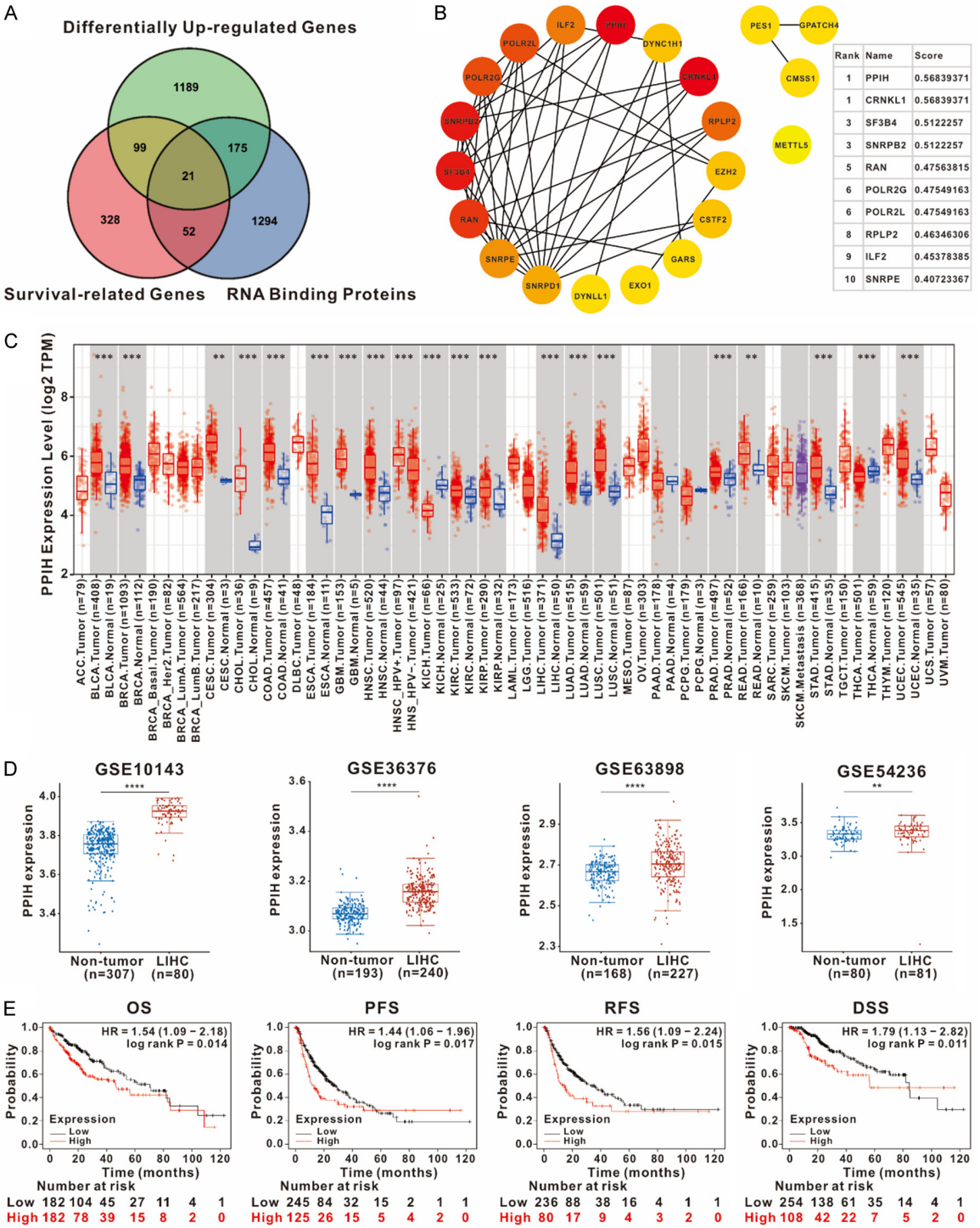

Figure 1. Identification of the target gene and its expression characteristics. A. Venn diagram illustrating the intersection of differentially upregulated genes, survival-related genes, and RBPs. B. Protein-protein interaction analysis of the 21 differential RBPs by using the STRING website (https://www.string-db.org/) and Cytoscape software. The table displays the top 10 genes identified using the DMNC algorithm. C. Differential expression patterns of PPIH across 33 types of tumors and adjacent normal tissues in the TCGA database. Box plots exhibit the distribution of gene expression levels. D. Analysis of PPIH expression in LIHC tissues versus nontumor tissues by using the GEO database, including GSE10143, GSE36376, GSE63898, and GSE54236 cohorts. E. Kaplan-Meier survival analysis of an integrated nomogram for PPIH with OS, PFS, RFS, and DSS in patients with LIHC from the Kaplan-Meier plotter database based on Affymetrix microarray. DMNC, density of the maximum neighborhood component; RBP, RNA-binding protein; GEO, Gene Expression Omnibus; OS, overall survival; PFS, progression-free survival; RFS, recurrence-free survival; DSS, disease-specific survival; LIHC, liver hepatocellular carcinoma; TCGA, The Cancer Genome Atlas Database; **P ≤ 0.01, ***P ≤ 0.001, ****P ≤ 0.0001.

the association between PPIH and LIHC progression through bioinformatics analysis [54, 55]. Our results further support the cancer-promoting role of PPIH in LIHC. The alignment of these findings encouraged us to delve deeper into underlying mechanisms of PPIH in LIHC.

Clinicopathological characteristics of PPIH in patients with LIHC

To investigate the effect of PPIH expression on patients with LIHC, we analyzed the expression of PPIH across different clinicopathological characteristics in the TCGA-LIHC cohort. Our findings revealed an increased PPIH expression level in primary liver cancer. Moreover, we noted a positive correlation between PPIH expression and the grade, stage, and nodal metastasis status of LIHC. These results indicate that the expression level of PPIH increases with the intensity of the malignancy of LIHC (**Figure 2A**). We examined the relationship between high PPIH expression and clinical risk factors in patients with liver cancer. Our results revealed that high PPIH expression was significantly associated with poor OS in the following patient groups: men (n = 246, HR = 1.99, 95% confidence interval [CI] = 1.26-3.14, P = 0.0027), Asians (n = 156, HR = 2.34, 95% CI = 1.25-4.36, P = 0.006), those who consumed alcohol (n = 115, HR = 2.12, 95% CI = 1.12-4.03, P = 0.0186), those with clinical stage 2+3 (n = 166, HR = 1.83, 95% CI = 1.14-2.94, P = 0.0109), those with clinical stage 3 (n = 83, HR = 2.23, 95% CI = 1.21-4.1, P = 0.0083), those with clinical stage 3+4 (n = 87, HR = 2.21, 95% CI = 1.23-3.98, P = 0.0068), and those with AJCC_T stage 3 (n = 78, HR = 2.16, 95% CI = 1.16-4.02, P = 0.0134; **Figure 2B**). In addition, both univariate and multivariate Cox regression analyses were conducted on PPIH expression and clinical factors, such as age, sex, race, pTNM stage, and pathological grading. These analyses revealed that PPIH expression significantly affected survival outcomes. Specifically, the analyses indicated that high PPIH expression was associated with worse OS (HR = 1.54, P = 0.014), PFS (HR = 1.44, P = 0.017), RFS (HR = 1.56, P = 0.015), and DSS (HR = 1.79, P = 0.011; **Figure 2C-F**). These results indicate that PPIH could serve as an independent prognostic factor that significantly predicts survival outcomes. These findings enhance our understanding of the role of PPIH in the development of LIHC and its effect on patient prognosis, providing valuable insights for personalized treatment and clinical decision-making. Further research is required to investigate the specific biological functions of PPIH and its potential therapeutic and prognostic applications in LIHC.

Correlation between PPIH and m6A methylation

RBPs perform various crucial functions within cells, including m6A RNA methylation modification, which affects the occurrence and progression of cancer by regulating gene expression [56]. We hypothesized that PPIH affects the function and stability of RNA by recognizing and regulating various RNA modifications. This regulation, in turn, alters the expression of specific genes, thus affecting the physiological state and function of cells. To investigate the potential mechanisms of PPIH in LIHC, we analyzed the methylation level of m6A in LIHC. We examined the expression profiles of m6A modification-related genes in hepatocellular carcinoma (n = 371) and normal tissues (n = 276) using data from the GTEx database and the TCGA-LIHC cohort. Our findings revealed that most m6A-related genes, including *IGF2BP3*, *IGF2BP1*, *IGF2BP2*, *WTAP*, *YTHDC1*, *RBM15*, *YTHDF2*, *RBM15B*, *YTHDF1*, *HNRNPC*, *RBMX*, *ALKBH5*, *METTL14*, *YTHDF3*, and *FTO*, were upregulated in LIHC. By contrast, *METTL3*, *HNRNPA2B1*, *ZC3H13*, and *YTHDC2* expression were upregulated in normal tissues (Figure S2A). These results suggest that m6A methylation modification plays a crucial role in the occurrence and development of LIHC. Next, we investigated the relationship between PPIH and m6A methylation-related genes in LIHC by analyzing data from 372 hepatocellular carcinoma cases (in FPKM format) from the TCGA-LIHC cohort in the GDC database. The cases were categorized into high and low expression groups for PPIH on the basis of the median PPIH expression value. Our analysis revealed that m6A-related genes were more highly expressed in the high PPIH expression group than in the low PPIH expression group, including *IGBF2BP3*, *IGF2BP1*, *IGF2BP2*, *ZC3H13*, *ALKBH5*, *VIRMA*, *METTL3*, *YTHDC1*, *HNRNPA2B1*, *HNRNPC*, *RBMX*, *RBM15B*, *YTHDF1*, *WTAP*, *RBM15*, and *YTHDF2* (**Figure 3A**). Then, we analyzed the correlation between PPIH and

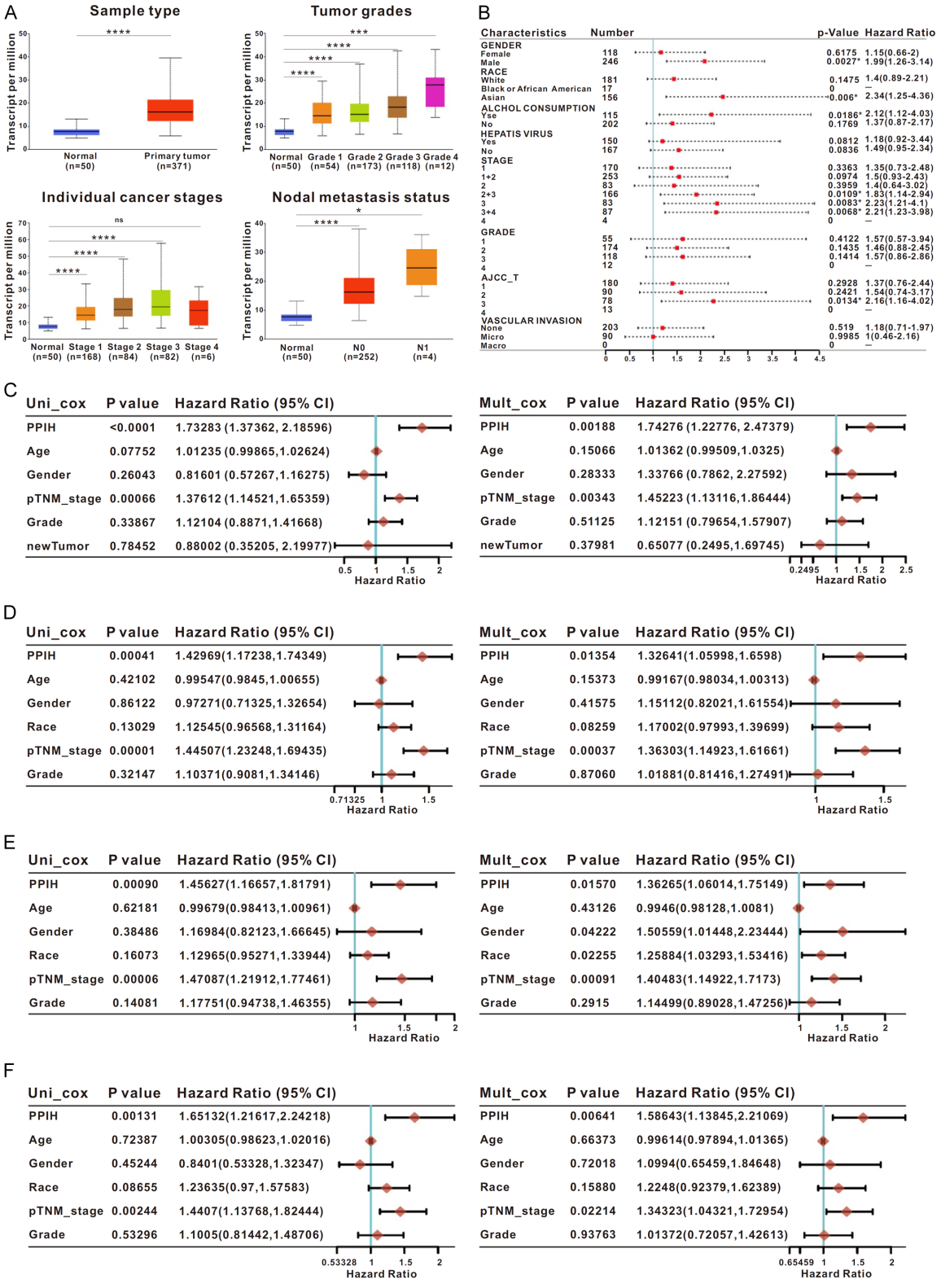

Figure 2. Clinicopathological characteristics of PPIH in patients with LIHC. (A) Association of PPIH expression with various clinicopathological characteristics within the TCGA-LIHC cohort, including sample type, tumor grades, individual cancer stages, and nodal metastasis status. (B) Relationship between PPIH expression and clinical risk factors in patients with LIHC. (C-F) Forest plots displaying the results of univariate and multivariate Cox regression analyses of PPIH expression and clinical features in patients with LIHC, assessing OS (C), PFS (D), DFS (E), and DSS (F). LIHC, liver hepatocellular carcinoma; OS, overall survival; PFS, progression-free survival; RFS, recurrence-free survival; DFS, disease-free survival; DSS, disease-specific survival.

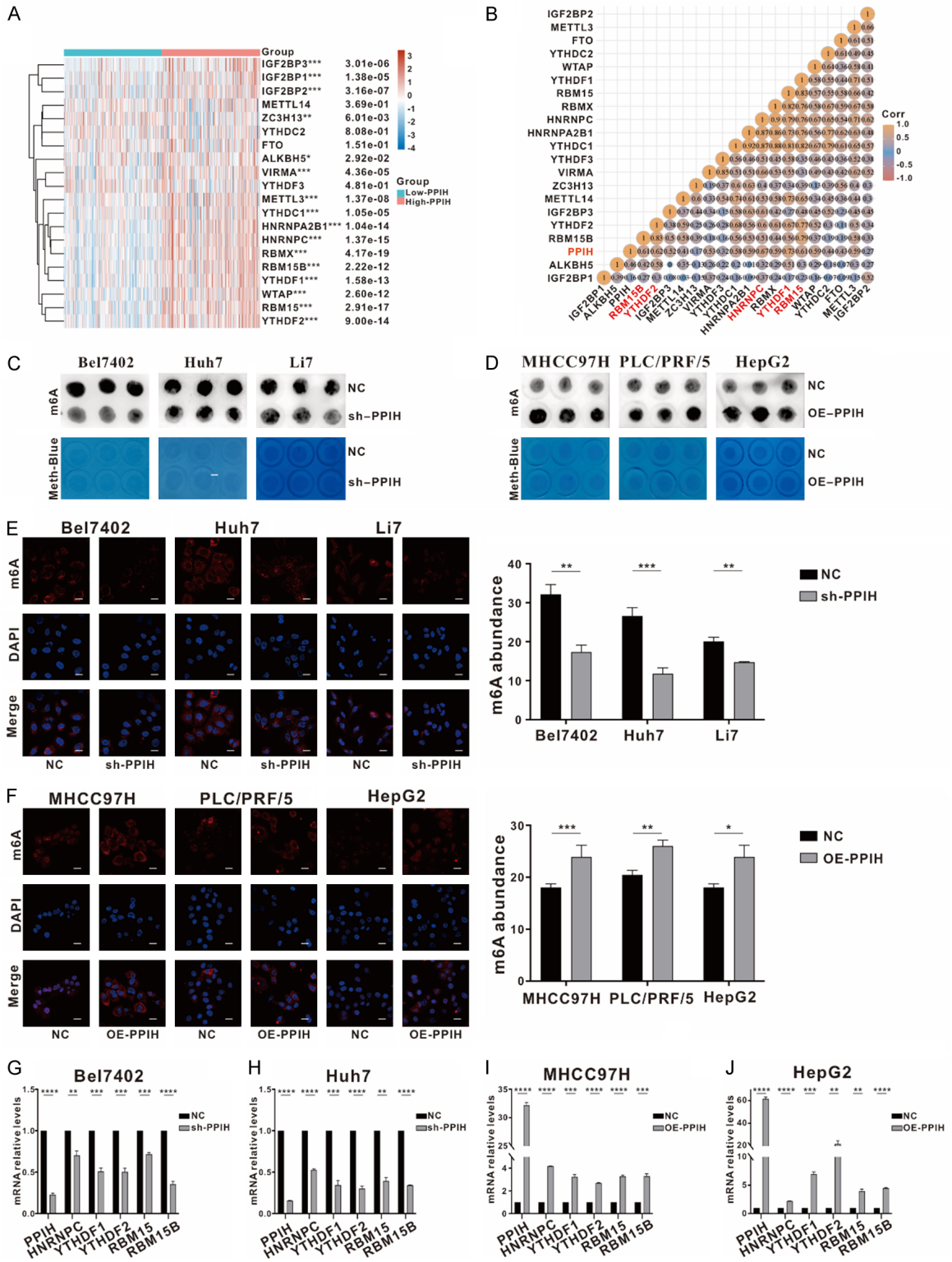

Figure 3. Effect of PPIH expression on the distribution of m6A methylation in LIHC. (A) Expression profiles of m6A modification-related genes in groups with low and high PPIH expression. (B) Correlation analysis between PPIH and m6A-related genes. (C, D) RNA dot blot analysis of the overall m6A methylation level in cells with PPIH knockdown (C) and (D) overexpression, with methylene blue serving as a loading control. (E, F) Immunofluorescence analysis of m6A abundance in cells with PPIH knockdown (E) and overexpression (F). Quantitative analysis of immunofluorescence staining was performed. Scale bar = 20 μM. (G, H) qPCR was used to detect the expression of m6A meth-

ylation–related genes in Bel7402 (G) and Huh7 (H) cells with PPIH knockdown. (I, J) qPCR was used to detect the expression of m6A methylation-related genes in MHCC97H (I) and HepG2 (J) cells with PPIH overexpression. qPCR, quantitative polymerase chain reaction; LIHC, liver hepatocellular carcinoma; ns represents not significant; *P < 0.05, ****P < 0.0001.

the aforementioned m6A-related genes. The results revealed a significant positive correlation between PPIH and m6A-related genes in LIHC (**Figure 3B**), indicating that PPIH may play a crucial role in m6A methylation modification.

To investigate the effect of PPIH on intracellular m6A methylation levels, we first transfected the 4 PPIH-knockdown plasmids in HEK293T cells to screen out the plasmid with the best knockdown efficiency (Figure S2B), and then we used the knockdown and overexpression plasmids to produced lentivirus and established stably expressed cell lines through lentivirus infection. We selected cell lines on the basis of the existing level of PPIH expression for targeted knockdown or overexpression experiments. Bel7402, Huh7, and Li7 cells were chosen to construct cell lines with stable PPIH knockdown, and MHCC97H, PLC/PRF/5, and HepG2 cells were used to construct cell lines with stable PPIH overexpression. The efficiency of PPIH knockdown and overexpression in cells was confirmed using WB and qPCR (Figure S2C-E). We quantified the overall m6A methylation level by performing dot blot assays in LIHC cell lines with either knocked down or overexpressed PPIH. The results revealed a significant reduction in the m6A methylation level in Bel7402, Huh7, and Li7 cells following PPIH knockdown (**Figure 3C**). By contrast, the m6A methylation level was increased in MHCC97H, PLC/PRF/5, and HepG2 cells with PPIH overexpression (**Figure 3D**). Furthermore, the results of immunofluorescence staining were consistent with those of dot blot assays. Immunofluorescence staining revealed that PPIH knockdown resulted in a decrease in the fluorescence intensity of m6A methylation (**Figure 3E**), whereas PPIH overexpression increased the fluorescence intensity of m6A methylation (**Figure 3F**). To further explore the potential mechanism of PPIH in m6A methylation, we selected key m6A genes that had a significant correlation (R > 0.6) with PPIH on the basis of the findings of our correlation analysis, including *HNRNPC*, *YTHDF1*, *YTHDF2*, *RBM15*, and *RBM15B*. We then verified the differences in the expression of these m6A-related genes between the low and high PPIH expression groups through qPCR. The results indicated that expression of m6A-related genes was significantly decreased in cells with PPIH knockdown (**Figure 3G**, **3H**), whereas expression of m6A-related genes was increased in cells with PPIH overexpression (**Figure 3I**, **3J**). This finding suggests that the expression of PPIH is synchronized with that of m6A methylation-related genes. Taken together, these findings suggest that PPIH increases the m6A RNA methylation level through the upregulation of m6A-related genes, thereby promoting LIHC progression.

Relationship between PPIH and tumor immune microenvironment

Previous studies have indicated that the role of RBPs in the tumor immune microenvironment is complex and diverse. RBPs affect the immune response by participating in various immunomodulatory mechanisms, including regulating the expression of T-cell receptors and costimulatory molecules, maintaining the differentiation and functional stability of immune cells, controlling the production of cytokines, and facilitating the presentation of antigens. Thus, RBPs play a key role in immune evasion and influence the effectiveness of tumor therapies [57-59]. Furthermore, m6A RNA modification regulates immunogenicity and antitumor responses [60]. Because PPIH increases the m6A modification level in LIHC cell lines, we hypothesized that PPIH is involved in regulating cancer immunity. To explore the relationship between PPIH and the LIHC tumor microenvironment, we analyzed the effect of the PPIH expression level on 10 types of immune-infiltrating cells in the TCGA-LIHC cohort by using the MCPcounter algorithm from the CAMOIP database. We determined that high PPIH expression was associated with an increased infiltration of immune and stromal cells, including T cells, $CD8^+$ T cells, cytotoxic lymphocytes, B lineage, monocytic lineage, myeloid dendritic cell, neutrophils, and endothelial cells. However, the increase in nat-

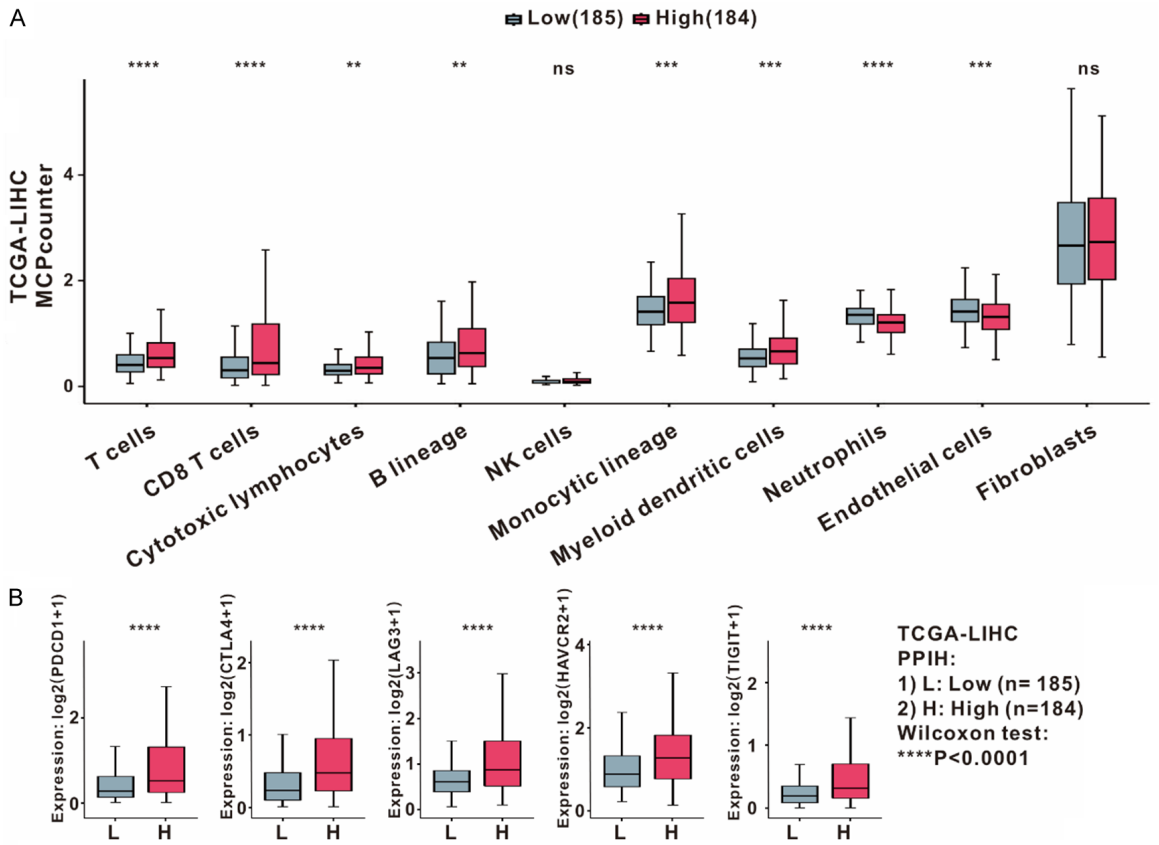

Figure 4. Effect of PPIH expression on the tumor microenvironment in the TCGA-LIHC cohort. A. Comparison of immune cell infiltration between the PPIH-low expression group (blue) and the PPIH-high expression group (red). B. Effects of PPIH expression on coinhibitory immune checkpoints, namely PD-1, CTLA4, LAG3, HAVCR2, and TIGIT. PD-1, programmed cell death-1; CTLA4, cytotoxic T-lymphocyte-associated protein 4; HAVCR2, hepatitis A virus cellular receptor 2; LAG3, lymphocyte-activation gene 3; TIGIT, T-cell immunoreceptor with Ig and ITIM domains; **P < 0.01, ***P < 0.001, ****P < 0.0001.

ural killer (NK) cells was not significant (**Figure 4A**). We speculated that PPIH upregulation in LIHC cells enables them to evade immune surveillance by NK cells, either by inhibiting the activation pathways of NK cells or by suppressing the expression of NK cell surface markers. Although PPIH upregulation leads to increased immune cell infiltration, our results indicated that high PPIH expression was associated with poor prognosis in LIHC. This adverse outcome may result from the presence of immunosuppressive cells and factors in the tumor microenvironment, including tumor-associated macrophages and regulatory T cells, which can suppress the antitumor effect of immune cells. Then, we further evaluated the correlation between PPIH and immune checkpoints. We observed that the expression of PPIH increased with that of classical coinhibitory immune checkpoints, namely PD-1, CTLA4, HAVCR2, LAG3, and TIGIT (**Figure 4B**). These findings suggest that PPIH affects the development and prognosis of LIHC by influencing immune cell infiltration or upregulating the expression of immune checkpoint proteins in the tumor microenvironment, indicating that PPIH may serve as a target for cancer immunotherapy in LIHC.

PPIH-related functional enrichment analysis

To investigate other potential biological mechanisms of PPIH in LIHC progression, we performed GSEA. In addition, functional enrichment analysis of PPIH was performed using HALLMARK and Kyoto Encyclopedia of Genes and Genomes (KEGG) databases. The top 10 significantly enriched signaling pathways were selected to create pathway enrichment plots. The results indicated that PPIH was significant-

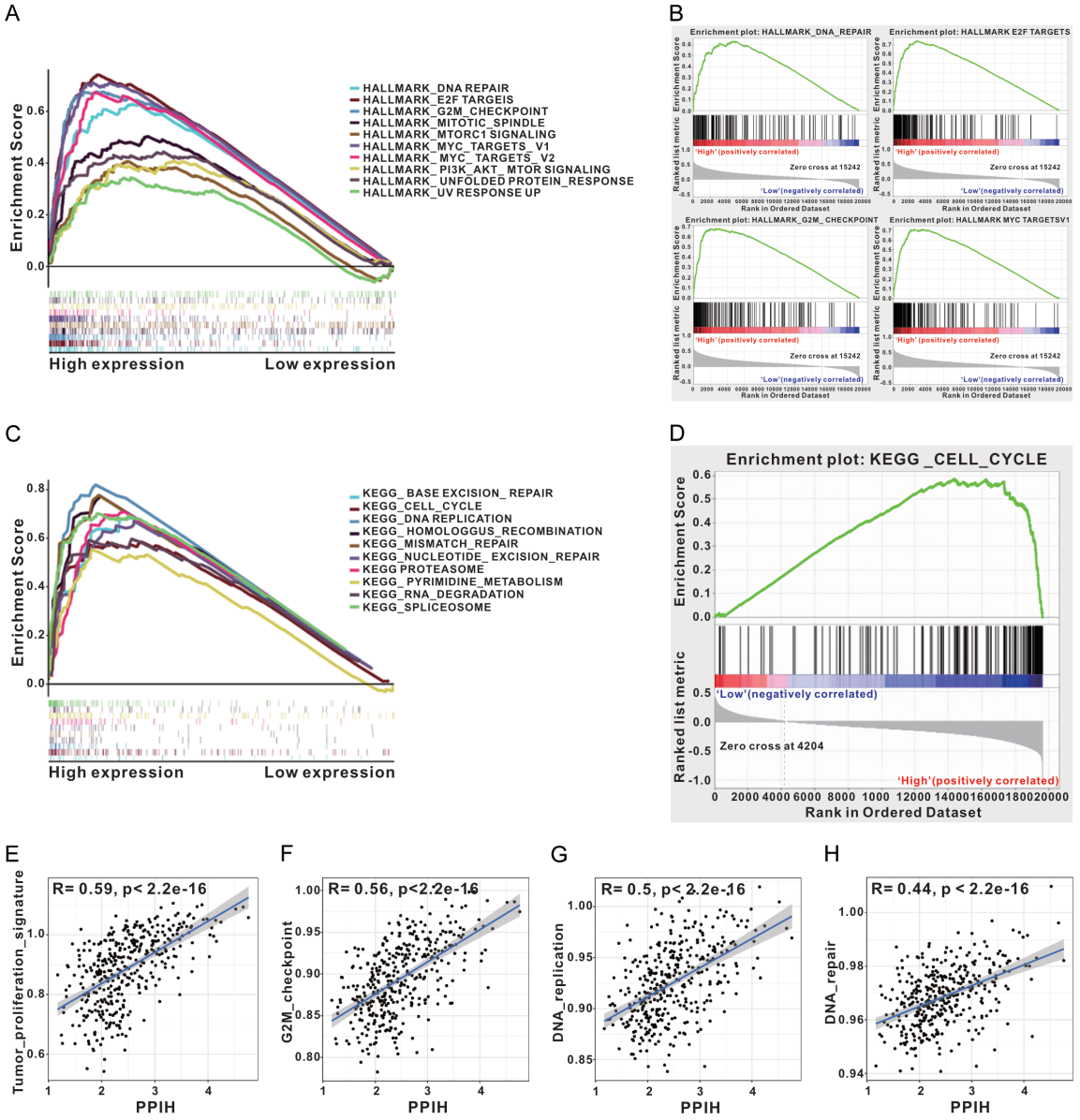

Figure 5. Functional enrichment analysis of PPIH. (A) GSEA was performed using the Hallmark gene set. (B) Hallmark enrichment results for "HALLMARK DNA repair", "HALLMARK E2F targets", "HALLMARK G2M checkpoint" and "HALLMARK MYC targets V1" from the GSEA. (C) GSEA based on the KEGG pathway database. (D) GSEA-based KEGG analysis of PPIH in cell cycle. (E-H) Scatter plots illustrating the correlation between PPIH and various signaling pathways, including tumor proliferation signature (E), G2M checkpoint (F), DNA replication (G), and DNA repair (H). The abscissa represents the distribution of gene expression, whereas the ordinate represents the distribution of pathway scores. GSEA, gene set enrichment analysis; KEGG, Kyoto Encyclopedia of Genes and Genomes.

ly enriched in signaling pathways related to DNA repair, E2F targets, G2M checkpoint, MYC targets, cell cycle, and DNA replication (**Figure 5A-D**). These signaling pathways are integral to cell proliferation and stemness. For example, E2F and G2M pathways play pivotal roles in cell cycle regulation. Previous studies have demonstrated that dosage-dependent copy number gains in E2F1 and E2F3 drive the development and progression of LIHC [61]. Furthermore, the G2/M checkpoint signaling pathway is critical for DNA damage response, cell cycle regulation, cell proliferation, and tumor progression [62]. The proto-oncogene *Myc* regulates multiple biological processes and plays critical roles in cell growth, proliferation, and cancer stem-

ness [63]. We examined the correlation between PPIH and gene signatures related to tumor proliferation (R = 0.59, P < 2.2e-16; **Figure 5E**), G2M cell cycle checkpoints (R = 0.56, P < 2.2e-16; **Figure 5F**), DNA replication (R = 0.56, P < 2.2e-16; **Figure 5G**), and DNA repair (R = 0.44, P < 2.2e-16; **Figure 5H**). The results indicated a significant positive correlation between PPIH expression and these critical signaling pathways, suggesting that PPIH promotes LIHC progression by modulating these malignant-related phenotypes.

PPIH promotes the cell cycle in LIHC cells

The findings of the functional enrichment analysis revealed that PPIH was significantly enriched in cell cycle signaling pathways. To investigate the effect of PPIH on cell cycle in LIHC, we used propidium iodide staining and fluorescence-activated cell sorting (FACS) to analyze the DNA content in control cells, PPIH knockdown cells, and PPIH overexpression cells. We calculated the percentages of cells in different phases of the cell cycle (G0/G1, S, and G2/M phases) in each group. Cells in the G0/G1 phase were typically quiescent, whereas those in the S and G2/M phases were actively proliferating. Compared with the negative control (NC) group, the Bel7402, Huh7, and Li7 cell lines exhibited a significant increase in the number of cells in the G0/G1 phase and a decrease in the number of cells in the S and G2/M phases following PPIH knockdown. This finding suggests that PPIH deficiency led to cell cycle arrest during the transition from the G0/G1 phase to the S phase (**Figure 6A-D**). By contrast, the MHCC97H, PLC/PRF/5, and HepG2 cell lines with PPIH overexpression exhibited a decrease in the number of cells in the G0/G1 phase but an increase in the number of cells in the S and G2/M phases, indicating that most cells were in a proliferative phase (**Figure 6E-H**). The results of FACS demonstrated the crucial role of PPIH in regulating the transition of LIHC cells from the G0/G1 phase to the S phase. To investigate specific mechanisms through which PPIH regulates the cell cycle, we performed qPCR to examine the relationship between PPIH and key cell cycle-related genes involved in the transition from the G1 phase to the S phase, including *cyclin A1* [64], *cyclin D1* [65], *P21* [66], and *P27* [67]. Cyclin A1 binds to cyclin-dependent kinase 2 to form an active complex that promotes the entry of cells into the S and G2/M phases [68]. Cyclin D1 interacts with CDK4/6 to drive the transition from the G1 phase to the S phase [69]. P21 and P27 regulate cell cycle progression by modulating the activity of CDKs [67, 70]. The results of qPCR revealed that the expression levels of *P21* and *P27* were significantly increased in Bel7402 cells with PPIH knockdown (**Figure 6I**). By contrast, in MHCC97H and PLC/PRF/5 cells with PPIH overexpression, the expression levels of *cyclin A1* and *cyclin D1* were significantly increased (**Figure 6J**, **6K**). These findings suggest that PPIH accelerates cell cycle by modulating the expression of cell cycle regulatory genes.

PPIH increases cell proliferation in LIHC cells

To confirm the effect of PPIH on LIHC cell proliferation, colony formation assays and cell growth curves measured by CCK-8 were used to assess cell viability and proliferation characteristics. Colony formation analysis revealed that PPIH knockdown significantly inhibited colony formation in Bel7402, Huh7, and Li7 cells compared with the NC (**Figure 7A**). By contrast, the overexpression of PPIH significantly increased the colony formation ability of MHCC97H, PLC/PRF/5, and HepG2 cells (**Figure 7B**). These results suggest that PPIH had a positive effect on the survival and proliferation of LIHC cells. Similarly, the cell growth curves exhibited comparable results. In Huh7 cells with PPIH knockdown, the growth curve showed a slower rate than did the NC (**Figure 7C**). By contrast, in PLC/PRF/5 cells with PPIH overexpression, the growth rate was significantly faster than that in the NC (**Figure 7D**), indicating that PPIH promotes the growth of LIHC cells. Next, we examined cell proliferative activity by using Edu staining combined with DAPI staining. Edu^+ cells, which indicate active DNA replication, were stained red by using Alexa Fluor 568. The nuclei of LIHC cells were stained blue with DAPI. The results demonstrated a significant decrease in the number of Edu^+ cells (proliferating cells) in Bel7402 and Huh7 cell lines with PPIH knockdown, indicating a significant reduction in proliferative activity (**Figure 7E**). By contrast, in MHCC97H and PLC/PRF/5 cells with PPIH overexpression, the

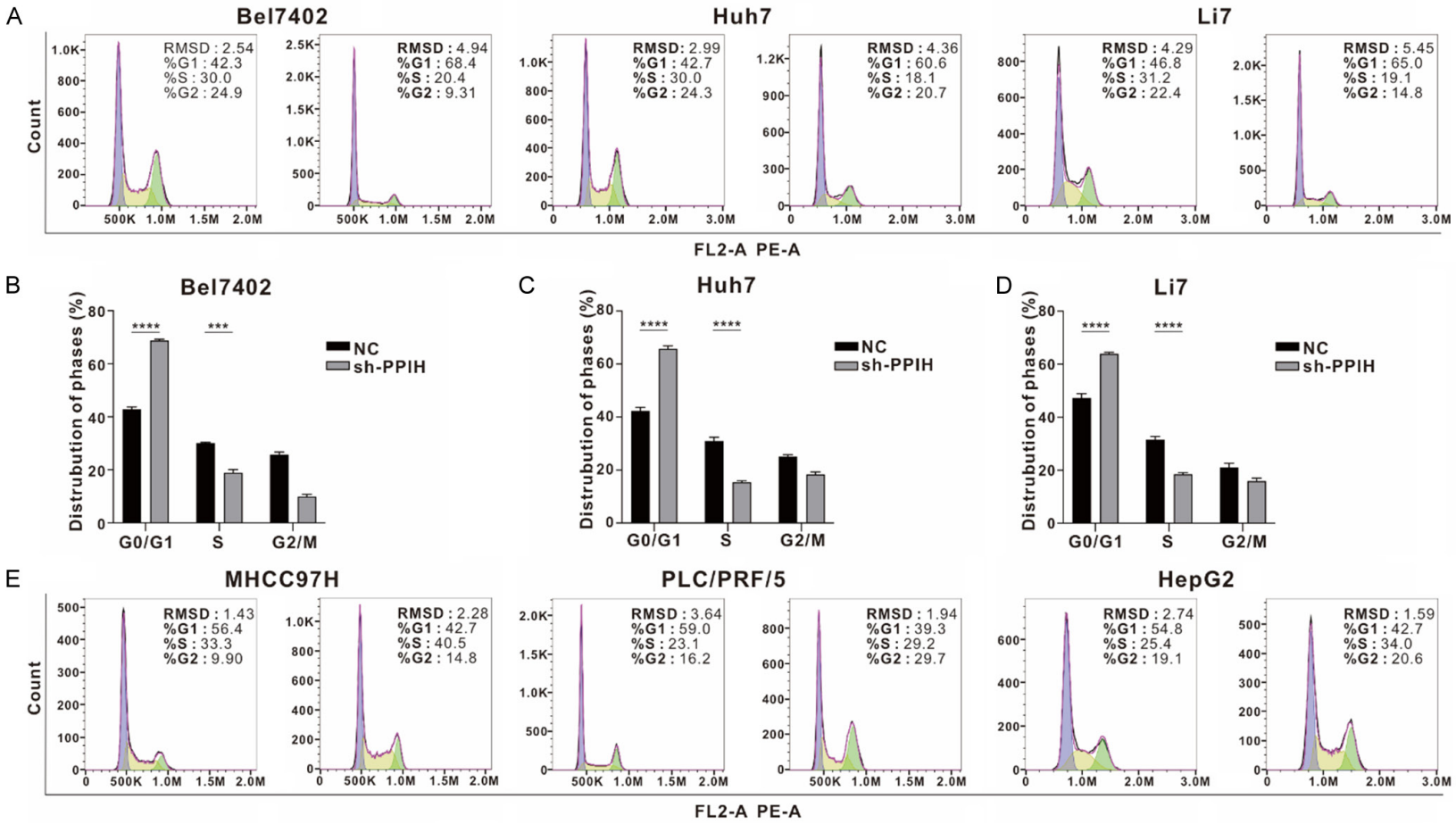
A
Bel7402
Huh7
Li7
Count
RMSD : 2.54
%G1 : 42.3
%S : 30.0
%G2 : 24.9
RMSD : 4.94
%G1 : 68.4
%S : 20.4
%G2 : 9.31
RMSD: 2.99
%G1 : 42.7
%S : 30.0
%G2 : 24.3
RMSD : 4.36
%G1 : 60.6
%S : 18.1
%G2 : 20.7
RMSD : 4.29
%G1 : 46.8
%S : 31.2
%G2 : 22.4
RMSD : 5.45
%G1 : 65.0
%S : 19.1
%G2 : 14.8
FL2-A PE-A
B
Bel7402
C
Huh7
D
Li7
Distrubution of phases (%)
NC
sh-PPIH
****
***
G0/G1
S
G2/M
E
MHCC97H
PLC/PRF/5
HepG2
RMSD : 1.43
%G1 : 56.4
%S : 33.3
%G2 : 9.90
RMSD : 2.28
%G1 : 42.7
%S : 40.5
%G2 : 14.8
RMSD : 3.64
%G1 : 59.0
%S : 23.1
%G2 : 16.2
RMSD : 1.94
%G1 : 39.3
%S : 29.2
%G2 : 29.7
RMSD : 2.74
%G1 : 54.8
%S : 25.4
%G2 : 19.1
RMSD : 1.59
%G1 : 42.7
%S : 34.0
%G2 : 20.6
FL2-A PE-A

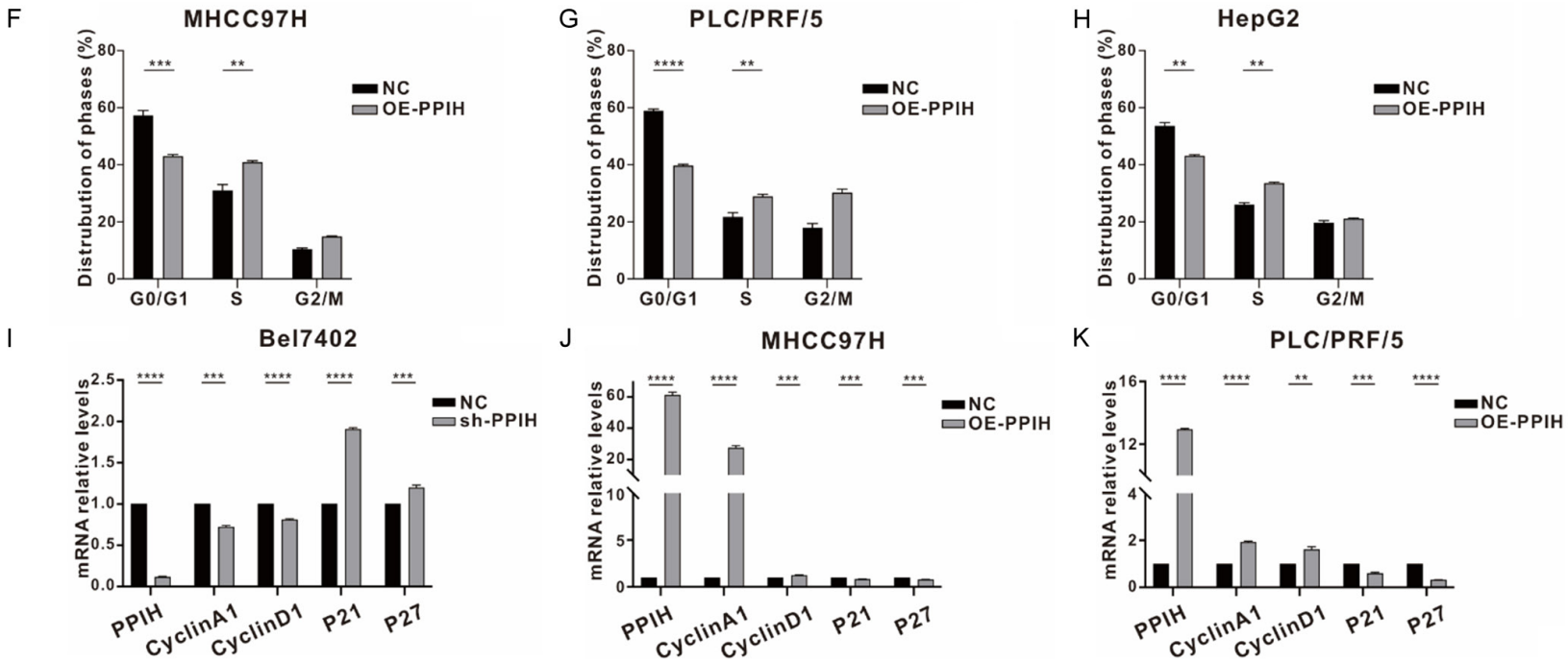

Figure 6. Effect of PPIH knockdown/overexpression on the cell cycle in LIHC. (A-D) Flow cytometry was used to analyze the cell cycle in PPIH knockdown cells from Bel7402, Huh7, and Li7 lines. Quantitative results are displayed. (E-H) Flow cytometry was performed to evaluate cell cycle in PPIH knockdown cells from MHCC97H, PLC/PRF/5, and HepG2 lines. Quantitative results are displayed. (I) qPCR was performed in Bel7402 cells with PPIH knockdown to analyze changes in cell cycle regulators. (J, K) qPCR was performed in MHCC97H (J) and PLC5/PRF/5 (K) with PPIH overexpression to analyze changes in cell cycle regulators. qPCR, quantitative polymerase chain reaction; LIHC, liver hepatocellular carcinoma; **P < 0.01, ***P < 0.001, ****P < 0.0001.

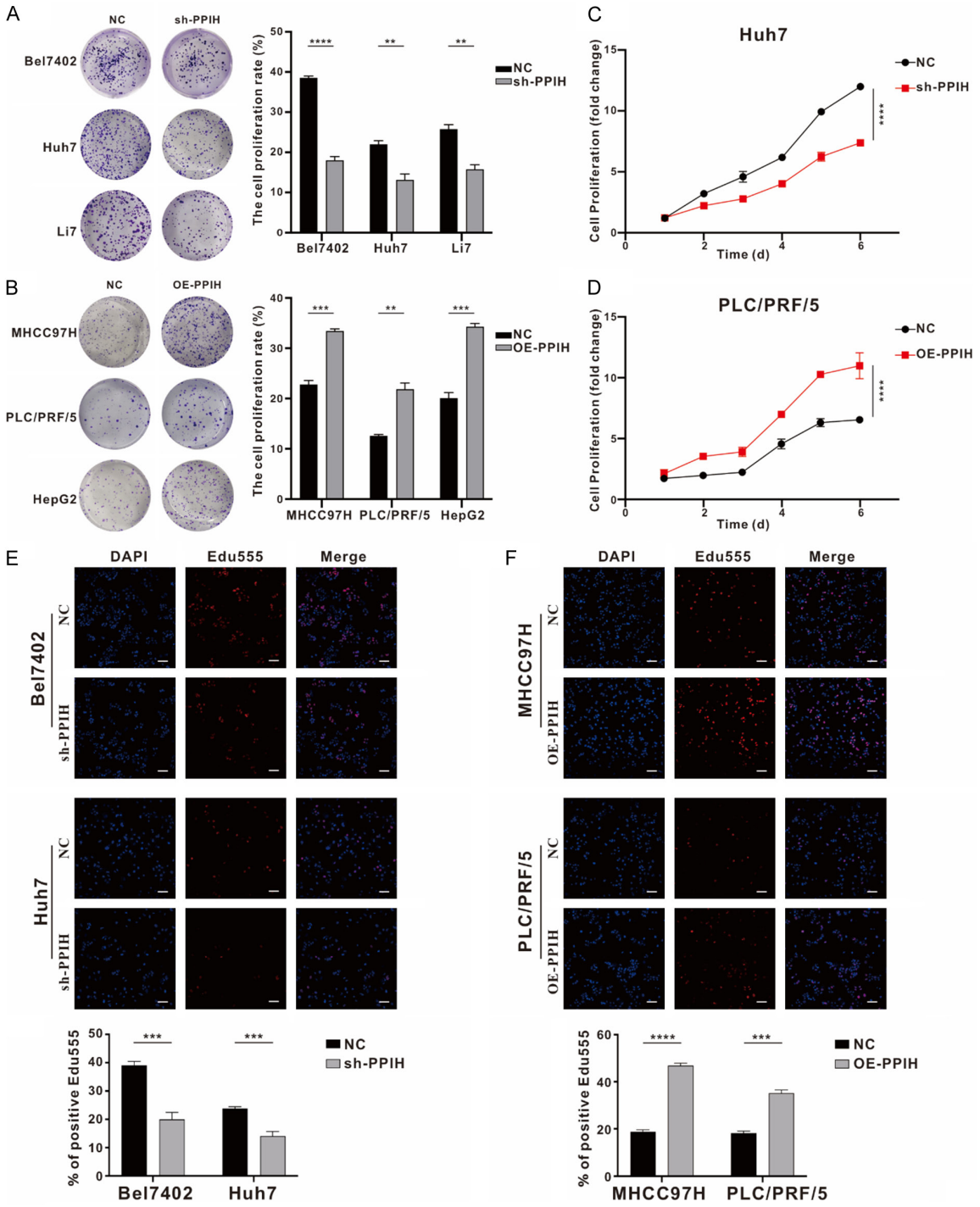

Figure 7. Effect of PPIH knockdown/overexpression on LIHC proliferation. (A, B) Colony formation assay was conducted to evaluate the colony-forming ability of PPIH knockdown cells. Quantitative results are displayed. (C, D) Growth curves of Huh7 (C) and PLC/PRF/5 (D) cells were determined using CCK-8. (E, F) Immunofluorescence analysis of Edu555 incorporation to assess the effect of PPIH expression on cell proliferation, $Edu555^{+}$ cells were stained red, and nuclei were stained blue, Scale bar = 100 μM. CCK-8, cell counting kit-8; LIHC, liver hepatocellular carcinoma; **P < 0.01, ***P < 0.001, ****P < 0.0001.

number of proliferating cells was significantly increased (**Figure 7F**). These in vitro results suggest that PPIH enhances the proliferative capacity of LIHC cells.

Discussion

Hepatocellular carcinoma is among the most common malignant tumors globally, and its incidence varies due to factors such as region, ethnicity, lifestyle habits, and disease prevalence [2]. The complex pathogenesis of LIHC, which involves various factors such as hepatitis virus infection, alcohol abuse, obesity, and fatty liver disease, complicates its treatment [4]. The occurrence and development of LIHC involves multiple biological processes, including tumor cell proliferation, invasion, metastasis, angiogenesis, and immune escape [3]. Current challenges in treating and managing LIHC include late-stage diagnosis, poor treatment outcomes, high recurrence rates, and drug resistance [2]. Thus, additional research and therapeutic innovations are required to improve the prognosis of patients with LIHC. Previous studies have indicated the crucial role of RBPs, such as HuR, PTBP1, SORBS2, RBM3, and RBPMS1, in LIHC. RBPs can regulate the expression of tumor-related genes, including those involved in proliferation and metastasis [10, 30, 31, 46, 51]. A previous study reported an association between PPIH and LIHC progression through bioinformatics analysis, and hypothesized that PPIH affects the development of LIHC through the spliceosome pathway [54]. Our results further support the oncogenic role of PPIH in LIHC and provide additional insights into complex molecular mechanisms through which PPIH contributes to LIHC pathogenesis and progression, prompting further investigation into the underlying mechanisms of PPIH in LIHC.

In the present study, we initially cross-referenced the upregulated gene set in LIHC with the survival-related gene set from the TCGA-LIHC cohort and the RBP data set and identified PPIH as the target gene. An analysis of the TCGA public database revealed that PPIH was highly expressed in various tumor tissues, especially LIHC, and its high expression was associated with poor prognosis. PPIH, a member of the prolyl isomerase (PPIase) family, is involved in various biological processes. PPIases participate in protein folding and assembly and regulate the stability, localization, and activity of mature proteins, thus affecting the structure and function of crucial cellular proteins, including tumor suppressor genes, proliferation factors, and apoptosis-related proteins, eventually affecting cell growth, differentiation, and apoptosis [71, 72]. In LIHC, aberrant protein conformation and stability can lead to the abnormal expression and dysfunction of tumor-related genes, thus facilitating tumor development and progression [73, 74]. PPIH, which possesses PPIase activity, may have specific functions and regulatory mechanisms that differ from others. However, PPIH shares the fundamental characteristics of PPIases in regulating protein conformation and stability [75]. In addition, as a crucial RBP, PPIH may play a vital role in the occurrence, development, and treatment of tumors. Research on the mechanisms of PPIH in tumors is ongoing, and a clear consensus has not yet been reached.

The results of this study indicated that PPIH was more highly expressed in LIHC tissues than in noncancerous tissues, suggesting the involvement of PPIH in the pathogenesis and development of LIHC. Further analysis revealed that the expression of PPIH was strongly associated with the clinical characteristics of LIHC, including tumor type, lymph node metastasis, and pathological grading. Univariate and multivariate Cox regression analyses of PPIH expression and clinical factors, namely age, sex, ethnicity, pTNM stage, and pathological grading, confirmed that PPIH is an independent risk factor for the prognosis of patients with LIHC. This finding indicates that PPIH can independently predict LIHC progression and mortality risk in patients with LIHC. Our study lays the groundwork for further validation of whether PPIH can serve as a potential prognostic biomarker for risk assessment, treatment planning, and clinical monitoring of patients with LIHC, which could ultimately improve their survival rate and quality of life.

As an RBP, PPIH may participate in recognizing and binding to m6A methylated sites on RNA molecules, thereby regulating RNA metabolism and functions, such as transcriptional regulation, RNA stability, translation, and degradation. These activities, in turn, affect crucial cellular processes, including gene expression, the cell cycle, and cell differentiation. We observed that high PPIH expression was associated with an increased expression of m6A-related genes and affected total m6A methylation levels with-

in LIHC cells. These findings suggest the presence of functional interactions or regulatory relationships between PPIH and m6A-related genes, indicating the involvement of PPIH in m6A RNA modification. Our study provides a critical clue for further exploration of the regulatory network between PPIH and the m6A modification mechanism. In addition, we examined the effect of PPIH on immune-infiltrating cells in the LIHC tumor microenvironment. We observed that PPIH increased immune cell infiltration in the tumor microenvironment and upregulated immune checkpoint gene expression. A previous study demonstrated that RNA m6A methylation modifications affect the tumor immune microenvironment by altering the expression of immunosuppressive molecules and T-cell infiltration [76]. Our study suggests that PPIH participates in immunomodulatory processes through the upregulation of immune checkpoints and RNA m6A methylation levels, thereby altering immune characteristics in the tumor microenvironment. However, these hypotheses require further validation in future studies.

As an important epigenetic modification, m6A is increasingly studied in hepatocellular carcinoma, particularly in cell proliferation [77]. In our study, PPIH promoted the proliferation of LIHC cells. We speculate that this may result from PPIH-mediated m6A methylation modifications regulating cell proliferation. There are several possible explanations for the this potential mechanisms. Firstly, m6A methylation-modifying enzyme such as FTO, WTAP and METTL3 are highly expressed in LIHC and related to the enhanced proliferation ability of tumor cells [21, 78, 79]. Our research indicates that PPIH can promote the expression levels of these m6A methylation-related enzymes, which may promote the proliferation of LIHC cells. Secondly, m6A methylation affects the expression of genes associated with liver cancer by regulating the mRNA stability, splicing, and translation efficiency. For example, m6A methylation can increase the expression of cell cycle regulatory proteins Cyclin D1 and CDK4, promoting the transition of cells from the G1 phase to the S phase, thereby accelerating the proliferation of LIHC cells [80]. We found that PPIH caused an overall increase in m6A methylation levels and promoted the expression of cell cycle proteins Cyclin A1 and Cyclin D1. Therefore, we hypothesize that PPIH-mediated m6A modifications promote the expression of cell cycle proteins and influence the progression of LIHC. Furthermore, m6A methylation regulates the proliferation of tumor cells by influencing gene expression in key signaling pathways. For instance, m6A modification can regulate the Wnt/β-catenin, Hippo, and PI3K/AKT/mTOR signaling pathways, which play critical roles in the growth and proliferation of cancer cells, thereby promoting tumor progression [81-84]. To sum up, we speculate that PPIH may play a positive role in the growth of hepatocellular carcinoma in an m6A-dependent manner. Further investigation into the functions and regulatory mechanisms of PPIH in LIHC could enhance our understanding of mechanisms underlying tumorigenesis and provide new targets or strategies for cancer treatment.

In conclusion, our study indicates the crucial role of PPIH in LIHC progression. PPIH regulates m6A methylation and affects immune cell infiltration in the tumor microenvironment. In addition, PPIH may promote cell proliferation by modulating DNA replication and the expression of cell cycle-related genes, thereby controlling cell cycle progression in LIHC. Ye J et al. have previously demonstrated that PPIH, a member of the cyclophilin family, is closely related to patients' survival and disease progression, suggesting its importance in predicting tumor prognosis [54, 85]. However, their research mainly focused on the predictive value of PPIH and lacked an in-depth exploration of its molecular mechanism and the exact action pathway. In this study, we used a combination of bioinformatics analysis, in vitro experiments, and data analysis to comprehensively analyze and validate the effects of PPIH, a member of the RNA-binding proteins, on m6A methylation, tumor immune microenvironment, and cell proliferation. We attempt to comprehensively understand the underlying mechanisms of PPIH in tumor prognosis and to provide a new perspective for understanding the progression of LIHC. Of course, our study has several limitations. For instance, the precise mechanism through which PPIH affects LIHC requires further exploration, and whether PPIH can also affect other malignant phenotypic indicators of LIHC need further investigation. Moreover, our conclusions are primarily based on analyses of

data from public databases and online bioinformatics tools, and our experiments were conducted in vitro. Further in vivo and clinical studies are needed to validate our findings.

Acknowledgements

This work was supported in part by the YingTsai Young Scholar Award (CMU108-YTY-04); the National Science and Technology Council Taiwan (NSTC 113-2320-B-039-017); the National Natural Science Foundation of China (82172789); the Science and Technology Project of Guangzhou Health Commission (No. 20241A011117); the Science and Technology Project of Panyu District, Guangzhou (No. 2023-Z04-021); the Internal Scientific Research Fund of Guangzhou Panyu Central Hospital (PY-2023-025); and the Science and Technology Project of Jiangsu Commission of Health (No. Z2022003).

Disclosure of conflict of interest

None.

Address correspondence to: Wen-Hao Yang, Graduate Institute of Cell Biology, and Cancer Biology and Precision Therapeutics Center, China Medical University, Taichung 404327, Taiwan. E-mail: why0331@gmail.com; Xiu-Wen Yan, Affiliated Cancer Hospital and Institute, Guangzhou Medical University, Guangzhou 510095, Guangdong, China. E-mail: sure83@163.com; Kai-Wen Hsu, Institute of Translational Medicine and New Drug Development, China Medical University, Taichung 404328, Taiwan. E-mail: kwhsu@mail.cmu.edu.tw

References

[1] Li C, Wang H, Chen R, Zhang H, Xu Y, Zhang B, Li Y, Zhang C, Yang Y, Wang X and Li X. Outcomes and recurrence patterns following curative hepatectomy for hepatocellular carcinoma patients with different China liver cancer staging. Am J Cancer Res 2022; 12: 907-921.

[2] Singal AG, Kanwal F and Llovet JM. Global trends in hepatocellular carcinoma epidemiology: implications for screening, prevention and therapy. Nat Rev Clin Oncol 2023; 20: 864-884.

[3] Vogel A, Meyer T, Sapisochin G, Salem R and Saborowski A. Hepatocellular carcinoma. Lancet 2022; 400: 1345-1362.

[4] McGlynn KA, Petrick JL and London WT. Global epidemiology of hepatocellular carcinoma: an emphasis on demographic and regional variability. Clin Liver Dis 2015; 19: 223-238.

[5] Liu X, Zhang P, Martin RC, Cui G, Wang G, Tan Y, Cai L, Lv G and Li Y. Lack of fibroblast growth factor 21 accelerates metabolic liver injury characterized by steatohepatities in mice. Am J Cancer Res 2016; 6: 1011-1025.

[6] Zhang Y, Ren H, Li J, Xue R, Liu H, Zhu Z, Pan C, Lin Y, Hu A, Gou P, Cai J, Zhou J, Zhu W and Shi X. Elevated HMGB1 expression induced by hepatitis B virus X protein promotes epithelial-mesenchymal transition and angiogenesis through STAT3/miR-34a/NF-κB in primary liver cancer. Am J Cancer Res 2021; 11: 479-494.

[7] Hsu WF, Lai HC, Chen SH, Su WP, Wang HW, Chen HY, Huang GT and Peng CY. Effect of metabolic dysfunction on the risk of liver-related events in patients cured of hepatitis C virus. Am J Cancer Res 2024; 14: 1914-1925.

[8] Li JH, Wang YC, Qin CD, Yao RR, Zhang R, Wang Y, Xie XY, Zhang L, Wang YH and Ren ZG. Over expression of hyaluronan promotes progression of HCC via CD44-mediated pyruvate kinase M2 nuclear translocation. Am J Cancer Res 2016; 6: 509-521.

[9] Mai Y, Liao C, Wang S, Zhou X, Meng L, Chen C, Qin Y and Deng G. High glucose-induced NCAPD2 upregulation promotes malignant phenotypes and regulates EMT via the Wnt/β-catenin signaling pathway in HCC. Am J Cancer Res 2024; 14: 1685-1711.

[10] Qi W, Gao C, Zhang L, Gao Z, Sui J, Han C and Sun D. MiR-3196, a p53-responsive microRNA, functions as a tumor suppressor in hepatocellular carcinoma by targeting FOXP4. Am J Cancer Res 2019; 9: 2665-2678.

[11] Jung SY, Park JI, Jeong JH, Song KH, Ahn J, Hwang SG, Kim J, Park JK, Lim DS and Song JY. Receptor interacting protein 1 knockdown induces cell death in liver cancer by suppressing STAT3/ATR activation in a p53-dependent manner. Am J Cancer Res 2022; 12: 2594-2611.

[12] Xue X, Dong L, Burke E, Xue L and Lu YJ. The interaction of p53 and DNA repair gene mutations and their impact on tumor mutation burden and immune response in human malignancies. Am J Cancer Res 2022; 12: 1866-1883.

[13] Tornesello ML, Buonaguro L, Tatangelo F, Botti G, Izzo F and Buonaguro FM. Mutations in TP53, CTNNB1 and PIK3CA genes in hepatocellular carcinoma associated with hepatitis B and hepatitis C virus infections. Genomics 2013; 102: 74-83.

[14] Wang W, Liu P, Lavrijsen M, Li S, Zhang R, Li S, van de Geer WS, van de Werken HJG, Peppelenbosch MP and Smits R. Evaluation of AXIN1 and AXIN2 as targets of tankyrase inhi-

bition in hepatocellular carcinoma cell lines. Sci Rep 2021; 11: 7470.
[15] Liu F, Wei YG, Luo LM, Wang WT, Yan LN, Wen TF, Xu MQ, Yang JY and Li B. Genetic variants of p21 and p27 and hepatocellular cancer risk in a Chinese Han population: a case-control study. Int J Cancer 2013; 132: 2056-2064.
[16] Nan YL, Hu YL, Liu ZK, Duan FF, Xu Y, Li S, Li T, Chen DF and Zeng XY. Relationships between cell cycle pathway gene polymorphisms and risk of hepatocellular carcinoma. World J Gastroenterol 2016; 22: 5558-5567.
[17] Chew V, Lai L, Pan L, Lim CJ, Li J, Ong R, Chua C, Leong JY, Lim KH, Toh HC, Lee SY, Chan CY, Goh BKP, Chung A, Chow PKH and Albani S. Delineation of an immunosuppressive gradient in hepatocellular carcinoma using high-dimensional proteomic and transcriptomic analyses. Proc Natl Acad Sci U S A 2017; 114: E5900-E5909.
[18] Garnelo M, Tan A, Her Z, Yeong J, Lim CJ, Chen J, Lim KH, Weber A, Chow P, Chung A, Ooi LL, Toh HC, Heikenwalder M, Ng IO, Nardin A, Chen Q, Abastado JP and Chew V. Interaction between tumour-infiltrating B cells and T cells controls the progression of hepatocellular carcinoma. Gut 2017; 66: 342-351.
[19] Lim CJ, Lee YH, Pan L, Lai L, Chua C, Wasser M, Lim TKH, Yeong J, Toh HC, Lee SY, Chan CY, Goh BK, Chung A, Heikenwälder M, Ng IO, Chow P, Albani S and Chew V. Multidimensional analyses reveal distinct immune microenvironment in hepatitis B virus-related hepatocellular carcinoma. Gut 2019; 68: 916-927.
[20] Nagaraju GP, Dariya B, Kasa P, Peela S and El-Rayes BF. Epigenetics in hepatocellular carcinoma. Semin Cancer Biol 2022; 86: 622-632.
[21] Chen M, Wei L, Law CT, Tsang FH, Shen J, Cheng CL, Tsang LH, Ho DW, Chiu DK, Lee JM, Wong CC, Ng IO and Wong CM. RNA N6-methyladenosine methyltransferase-like 3 promotes liver cancer progression through YTHDF2-dependent posttranscriptional silencing of SOCS2. Hepatology 2018; 67: 2254-2270.
[22] Lin Z, Niu Y, Wan A, Chen D, Liang H, Chen X, Sun L, Zhan S, Chen L, Cheng C, Zhang X, Bu X, He W and Wan G. RNA m(6) A methylation regulates sorafenib resistance in liver cancer through FOXO3-mediated autophagy. EMBO J 2020; 39: e103181.
[23] Yang Y, Yan Y, Yin J, Tang N, Wang K, Huang L, Hu J, Feng Z, Gao Q and Huang A. O-GlcNAcylation of YTHDF2 promotes HBV-related hepatocellular carcinoma progression in an N(6)-methyladenosine-dependent manner. Signal Transduct Target Ther 2023; 8: 63.
[24] Cheng H, Sun G, Chen H, Li Y, Han Z, Li Y, Zhang P, Yang L and Li Y. Trends in the treatment of advanced hepatocellular carcinoma: immune checkpoint blockade immunotherapy and related combination therapies. Am J Cancer Res 2019; 9: 1536-1545.
[25] Jia CC, Chen YH, Cai XR, Li Y, Zheng XF, Yao ZC, Zhao LY, Qiu DB, Xie SJ, Chen WJ, Liu C, Liu QL, Wu XY, Wang TT and Zhang Q. Efficacy of cytokine-induced killer cell-based immunotherapy for hepatocellular carcinoma. Am J Cancer Res 2019; 9: 1254-1265.
[26] Li JH, Wang Y, Xie XY, Yin X, Zhang L, Chen RX and Ren ZG. Aspirin in combination with TACE in treatment of unresectable HCC: a matched-pairs analysis. Am J Cancer Res 2016; 6: 2109-2116.
[27] Shi X, O'Neill C, Wang X, Chen Y, Yu Y, Tan M, Lv G, Li Y and Martin RC. Irreversible electroporation enhances immunotherapeutic effect in the off-target tumor in a murine model of orthotopic HCC. Am J Cancer Res 2021; 11: 3304-3319.
[28] Zhou ZJ, Dai Z, Zhou SL, Fu XT, Zhao YM, Shi YH, Zhou J and Fan J. Overexpression of HnRNP A1 promotes tumor invasion through regulating CD44v6 and indicates poor prognosis for hepatocellular carcinoma. Int J Cancer 2013; 132: 1080-1089.
[29] Zhu H, Berkova Z, Mathur R, Sehgal L, Khashab T, Tao RH, Ao X, Feng L, Sabichi AL, Blechacz B, Rashid A and Samaniego F. HuR suppresses fas expression and correlates with patient outcome in liver cancer. Mol Cancer Res 2015; 13: 809-818.
[30] Dong W, Dai ZH, Liu FC, Guo XG, Ge CM, Ding J, Liu H and Yang F. The RNA-binding protein RBM3 promotes cell proliferation in hepatocellular carcinoma by regulating circular RNA SCD-circRNA 2 production. EBioMedicine 2019; 45: 155-167.
[31] Tao S, Xie SJ, Diao LT, Lv G, Hou YR, Hu YX, Xu WY, Du B and Xiao ZD. RNA-binding protein CCDC137 activates AKT signaling and promotes hepatocellular carcinoma through a novel non-canonical role of DGCR8 in mRNA localization. J Exp Clin Cancer Res 2023; 42: 194.
[32] Miao B, Wei C, Qiao Z, Han W, Chai X, Lu J, Gao C, Dong R, Gao D, Huang C, Ke A, Zhou J, Fan J, Shi G, Lan F and Cai J. eIF3a mediates HIF1α-dependent glycolytic metabolism in hepatocellular carcinoma cells through translational regulation. Am J Cancer Res 2019; 9: 1079-1090.
[33] Song Y, He S, Ma X, Zhang M, Zhuang J, Wang G, Ye Y and Xia W. RBMX contributes to hepatocellular carcinoma progression and sorafenib resistance by specifically binding and stabilizing BLACAT1. Am J Cancer Res 2020; 10: 3644-3665.

[34] Gerstberger S, Hafner M and Tuschl T. A census of human RNA-binding proteins. Nat Rev Genet 2014; 15: 829-845.
[35] Hentze MW, Castello A, Schwarzl T and Preiss T. A brave new world of RNA-binding proteins. Nat Rev Mol Cell Biol 2018; 19: 327-341.
[36] Qin H, Ni H, Liu Y, Yuan Y, Xi T, Li X and Zheng L. RNA-binding proteins in tumor progression. J Hematol Oncol 2020; 13: 90.
[37] Birsa N, Bentham MP and Fratta P. Cytoplasmic functions of TDP-43 and FUS and their role in ALS. Semin Cell Dev Biol 2020; 99: 193-201.
[38] Igarashi A, Itoh K, Yamada T, Adachi Y, Kato T, Murata D, Sesaki H and Iijima M. Nuclear PTEN deficiency causes microcephaly with decreased neuronal soma size and increased seizure susceptibility. J Biol Chem 2018; 293: 9292-9300.
[39] Murphy JJ, Surendranath K and Kanagaraj R. RNA-binding proteins and their emerging roles in cancer: beyond the tip of the iceberg. Int J Mol Sci 2023; 24: 9612.
[40] Wang X, Wang J, Tsui YM, Shi C, Wang Y, Zhang X, Yan Q, Chen M, Jiang C, Yuan YF, Wong CM, Liu M, Feng ZY, Chen H, Ng IOL, Jiang L and Guan XY. RALYL increases hepatocellular carcinoma stemness by sustaining the mRNA stability of TGF-β2. Nat Commun 2021; 12: 1518.
[41] Feng M, Xie X, Han G, Zhang T, Li Y, Li Y, Yin R, Wang Q, Zhang T, Wang P, Hu J, Cheng Y, Gao Z, Wang J, Chang J, Cui M, Gao K, Chai J, Liu W, Guo C, Li S, Liu L, Zhou F, Chen J and Zhang H. YBX1 is required for maintaining myeloid leukemia cell survival by regulating BCL2 stability in an m6A-dependent manner. Blood 2021; 138: 71-85.
[42] Zhang L, Chen Y, Li C, Liu J, Ren H, Li L, Zheng X, Wang H and Han Z. RNA binding protein PUM2 promotes the stemness of breast cancer cells via competitively binding to neuropilin-1 (NRP-1) mRNA with miR-376a. Biomed Pharmacother 2019; 114: 108772.
[43] Ji L, Li X, Zhou Z, Zheng Z, Jin L and Jiang F. LINC01413/hnRNP-K/ZEB1 axis accelerates cell proliferation and EMT in colorectal cancer via inducing YAP1/TAZ1 translocation. Mol Ther Nucleic Acids 2020; 19: 546-561.
[44] Lee WJ, Shin CH, Ji H, Jeong SD, Park MS, Won HH, Pandey PR, Tsitsipatis D, Gorospe M and Kim HH. hnRNPK-regulated LINC00263 promotes malignant phenotypes through miR-147a/CAPN2. Cell Death Dis 2021; 12: 290.
[45] Pan H, Strickland A, Madhu V, Johnson ZI, Chand SN, Brody JR, Fertala A, Zheng Z, Shapiro IM and Risbud MV. RNA binding protein HuR regulates extracellular matrix gene expression and pH homeostasis independent of controlling HIF-1α signaling in nucleus pulposus cells. Matrix Biol 2019; 77: 23-40.
[46] Liu L, Christodoulou-Vafeiadou E, Rao JN, Zou T, Xiao L, Chung HK, Yang H, Gorospe M, Kontoyiannis D and Wang JY. RNA-binding protein HuR promotes growth of small intestinal mucosa by activating the Wnt signaling pathway. Mol Biol Cell 2014; 25: 3308-3318.
[47] Bell JL, Wächter K, Mühleck B, Pazaitis N, Köhn M, Lederer M and Hüttelmaier S. Insulin-like growth factor 2 mRNA-binding proteins (IGF2BPs): post-transcriptional drivers of cancer progression? Cell Mol Life Sci 2013; 70: 2657-2675.
[48] Nagaoka K, Fujii K, Zhang H, Usuda K, Watanabe G, Ivshina M and Richter JD. CPEB1 mediates epithelial-to-mesenchyme transition and breast cancer metastasis. Oncogene 2016; 35: 2893-2901.
[49] Fu J, Cheng L, Wang Y, Yuan P, Xu X, Ding L, Zhang H, Jiang K, Song H, Chen Z and Ye Q. The RNA-binding protein RBPMS1 represses AP-1 signaling and regulates breast cancer cell proliferation and migration. Biochim Biophys Acta 2015; 1853: 1-13.
[50] Zhou Y, Huang T, Siu HL, Wong CC, Dong Y, Wu F, Zhang B, Wu WK, Cheng AS, Yu J, To KF and Kang W. IGF2BP3 functions as a potential oncogene and is a crucial target of miR-34a in gastric carcinogenesis. Mol Cancer 2017; 16: 77.
[51] Shen L, Lei S, Zhang B, Li S, Huang L, Czachor A, Breitzig M, Gao Y, Huang M, Mo X, Zheng Q, Sun H and Wang F. Skipping of exon 10 in Axl pre-mRNA regulated by PTBP1 mediates invasion and metastasis process of liver cancer cells. Theranostics 2020; 10: 5719-5735.
[52] Jiang F, Hedaya OM, Khor E, Wu J, Auguste M and Yao P. RNA binding protein PRRC2B mediates translation of specific mRNAs and regulates cell cycle progression. Nucleic Acids Res 2023; 51: 5831-5846.
[53] Shen L, Liang Z and Yu H. Dot blot analysis of N(6)-methyladenosine RNA modification levels. Bio Protoc 2017; 7: e2095.
[54] Ye J, Pang Y, Yang X, Zhang C, Shi L, Chen Z, Huang G, Wang X and Lu F. PPIH gene regulation system and its prognostic significance in hepatocellular carcinoma: a comprehensive analysis. Aging (Albany NY) 2023; 15: 11448-11470.
[55] Li M, Liu Z, Wang J, Liu H, Gong H, Li S, Jia M and Mao Q. Systematic analysis identifies a specific RNA-binding protein-related gene model for prognostication and risk-adjustment in HBV-related hepatocellular carcinoma. Front Genet 2021; 12: 707305.
[56] Huang H, Weng H, Sun W, Qin X, Shi H, Wu H, Zhao BS, Mesquita A, Liu C, Yuan CL, Hu YC,

Hüttelmaier S, Skibbe JR, Su R, Deng X, Dong L, Sun M, Li C, Nachtergaele S, Wang Y, Hu C, Ferchen K, Greis KD, Jiang X, Wei M, Qu L, Guan JL, He C, Yang J and Chen J. Recognition of RNA N(6)-methyladenosine by IGF2BP proteins enhances mRNA stability and translation. Nat Cell Biol 2018; 20: 285-295.

[57] Jeltsch KM and Heissmeyer V. Regulation of T cell signaling and autoimmunity by RNA-binding proteins. Curr Opin Immunol 2016; 39: 127-135.

[58] Zhao R, Peng C, Song C, Zhao Q, Rong J, Wang H, Ding W, Wang F and Xie Y. BICC1 as a novel prognostic biomarker in gastric cancer correlating with immune infiltrates. Int Immunopharmacol 2020; 87: 106828.

[59] Hashimoto S and Kishimoto T. Roles of RNA-binding proteins in immune diseases and cancer. Semin Cancer Biol 2022; 86: 310-324.

[60] Li X, Ma S, Deng Y, Yi P and Yu J. Targeting the RNA m(6)A modification for cancer immunotherapy. Mol Cancer 2022; 21: 76.

[61] Kent LN, Bae S, Tsai SY, Tang X, Srivastava A, Koivisto C, Martin CK, Ridolfi E, Miller GC, Zorko SM, Plevris E, Hadjiyannis Y, Perez M, Nolan E, Kladney R, Westendorp B, de Bruin A, Fernandez S, Rosol TJ, Pohar KS, Pipas JM and Leone G. Dosage-dependent copy number gains in E2f1 and E2f3 drive hepatocellular carcinoma. J Clin Invest 2017; 127: 830-842.

[62] Yin L, Chang C and Xu C. G2/M checkpoint plays a vital role at the early stage of HCC by analysis of key pathways and genes. Oncotarget 2017; 8: 76305-76317.

[63] Smith BAH, Deutzmann A, Correa KM, Delaveris CS, Dhanasekaran R, Dove CG, Sullivan DK, Wisnovsky S, Stark JC, Pluvinage JV, Swaminathan S, Riley NM, Rajan A, Majeti R, Felsher DW and Bertozzi CR. MYC-driven synthesis of Siglec ligands is a glycoimmune checkpoint. Proc Natl Acad Sci U S A 2023; 120: e2215376120.

[64] Ji P, Agrawal S, Diederichs S, Bäumer N, Becker A, Cauvet T, Kowski S, Beger C, Welte K, Berdel WE, Serve H and Müller-Tidow C. Cyclin A1, the alternative A-type cyclin, contributes to G1/S cell cycle progression in somatic cells. Oncogene 2005; 24: 2739-2744.

[65] Yu X, Pang L, Yang T and Liu P. lncRNA LINC01296 regulates the proliferation, metastasis and cell cycle of osteosarcoma through cyclin D1. Oncol Rep 2018; 40: 2507-2514.

[66] King ML and Murphy LL. Role of cyclin inhibitor protein p21 in the inhibition of HCT116 human colon cancer cell proliferation by American ginseng (Panax quinquefolius) and its constituents. Phytomedicine 2010; 17: 261-268.

[67] Pillay K, McCleod H, Chetty R and Hall P. A study to investigate the role of p27 and cyclin E immunoexpression as a prognostic factor in early breast carcinoma. World J Surg Oncol 2011; 9: 31.

[68] Tian RQ, Wang XH, Hou LJ, Jia WH, Yang Q, Li YX, Liu M, Li X and Tang H. MicroRNA-372 is down-regulated and targets cyclin-dependent kinase 2 (CDK2) and cyclin A1 in human cervical cancer, which may contribute to tumorigenesis. J Biol Chem 2011; 286: 25556-25563.

[69] Topacio BR, Zatulovskiy E, Cristea S, Xie S, Tambo CS, Rubin SM, Sage J, Kõivomägi M and Skotheim JM. Cyclin D-Cdk4,6 drives cell-cycle progression via the retinoblastoma protein's C-terminal helix. Mol Cell 2019; 74: 758-770, e754.

[70] Jiang D, Wang X, Liu X and Li F. Gene delivery of cyclin-dependent kinase inhibitors p21Waf1 and p27Kip1 suppresses proliferation of MCF-7 breast cancer cells in vitro. Breast Cancer 2014; 21: 614-623.

[71] Dunyak BM and Gestwicki JE. Peptidyl-proline isomerases (PPIases): targets for natural products and natural product-inspired compounds. J Med Chem 2016; 59: 9622-9644.

[72] Hanes SD. Prolyl isomerases in gene transcription. Biochim Biophys Acta 2015; 1850: 2017-2034.

[73] Zubiete-Franco I, García-Rodríguez JL, Lopitz-Otsoa F, Serrano-Macia M, Simon J, Fernández-Tussy P, Barbier-Torres L, Fernández-Ramos D, Gutiérrez-de-Juan V, López de Davalillo S, Carlevaris O, Beguiristain Gómez A, Villa E, Calvisi D, Martín C, Berra E, Aspichueta P, Beraza N, Varela-Rey M, Ávila M, Rodríguez MS, Mato JM, Díaz-Moreno I, Díaz-Quintana A, Delgado TC and Martínez-Chantar ML. SUMOylation regulates LKB1 localization and its oncogenic activity in liver cancer. EBioMedicine 2019; 40: 406-421.

[74] Gao W, Jia Z, Tian Y, Yang P, Sun H, Wang C, Ding Y, Zhang M, Zhang Y, Yang D, Tian Z, Zhou J, Ruan Z, Wu Y and Ni B. HBx protein contributes to liver carcinogenesis by H3K4me3 modification through stabilizing WD repeat domain 5 protein. Hepatology 2020; 71: 1678-1695.

[75] Thapar R. Roles of prolyl isomerases in RNA-mediated gene expression. Biomolecules 2015; 5: 974-999.

[76] Han D, Liu J, Chen C, Dong L, Liu Y, Chang R, Huang X, Liu Y, Wang J, Dougherty U, Bissonnette MB, Shen B, Weichselbaum RR, Xu MM and He C. Anti-tumour immunity controlled through mRNA m(6)A methylation and YTHDF1 in dendritic cells. Nature 2019; 566: 270-274.

[77] Chen M and Wong CM. The emerging roles of N6-methyladenosine (m6A) deregulation in liver carcinogenesis. Mol Cancer 2020; 19: 44.

[78] Chen Y, Peng C, Chen J, Chen D, Yang B, He B, Hu W, Zhang Y, Liu H, Dai L, Xie H, Zhou L, Wu

J and Zheng S. WTAP facilitates progression of hepatocellular carcinoma via m6A-HuR-dependent epigenetic silencing of ETS1. Mol Cancer 2019; 18: 127.

[79] Li J, Zhu L, Shi Y, Liu J, Lin L and Chen X. m6A demethylase FTO promotes hepatocellular carcinoma tumorigenesis via mediating PKM2 demethylation. Am J Transl Res 2019; 11: 6084-6092.

[80] Wang S, Sun C, Li J, Zhang E, Ma Z, Xu W, Li H, Qiu M, Xu Y, Xia W, Xu L and Yin R. Roles of RNA methylation by means of N6-methyladenosine (m6A) in human cancers. Cancer Lett 2017; 408: 112-120.

[81] Liu J, Eckert MA, Harada BT, Liu SM, Lu Z, Yu K, Tienda SM, Chryplewicz A, Zhu AC, Yang Y, Huang JT, Chen SM, Xu ZG, Leng XH, Yu XC, Cao J, Zhang Z, Liu J, Lengyel E and He C. m6A mRNA methylation regulates AKT activity to promote the proliferation and tumorigenicity of endometrial cancer. Nat Cell Biol 2018; 20: 1074-1083.

[82] Wang W, Shao F, Yang X, Wang J, Zhu R, Yang Y, Zhao G, Guo D, Sun Y, Wang J, Xue Q, Gao S, Gao Y, He J and Lu Z. METTL3 promotes tumour development by decreasing APC expression mediated by APC mRNA N(6)-methyladenosine-dependent YTHDF binding. Nat Commun 2021; 12: 3803.

[83] Du A, Li S, Zhou Y, Disoma C, Liao Y, Zhang Y, Chen Z, Yang Q, Liu P, Liu S, Dong Z, Razzaq A, Tao S, Chen X, Liu Y, Xu L, Zhang Q, Li S, Peng J and Xia Z. M6A-mediated upregulation of circMDK promotes tumorigenesis and acts as a nanotherapeutic target in hepatocellular carcinoma. Mol Cancer 2022; 21: 109.

[84] Wang J, Yu H, Dong W, Zhang C, Hu M, Ma W, Jiang X, Li H, Yang P and Xiang D. N6-methyladenosine-mediated up-regulation of FZD10 regulates liver cancer stem cells' properties and lenvatinib resistance through WNT/β-catenin and hippo signaling pathways. Gastroenterology 2023; 164: 990-1005.

[85] Ye J, Ying J, Chen H, Wu Z, Huang C, Zhang C, Chen Z and Chen H. PPIH acts as a potential predictive biomarker for patients with common solid tumors. BMC Cancer 2024; 24: 681.

Table S1. The sequence of short hairpin RNA directed against PPIH

Plasmid	Primer
pLKO.1-copGFP-PURO-NC	-
shPPIH-1	CCGGGTGATGAGAAAGATTGAGAATCTCGAGATTCTCAATCTTTCTCATCACTTTTTT
shPPIH-2	CCGGCGAACAGTGGTCCAAGTACAACTCGAGTTGTACTTGGACCACTGTTCGTTTTTT
shPPIH-3	CCGGCCACAGGGTCATAAAGGATTTCTCGAGAAATCCTTTATGACCCTGTGGTTTTTT
shPPIH-4	CCGGGTGTTCTTTGATGTCAGTATTCTCGAGAATACTGACATCAAAGAACACTTTTTT

Table S2. The primer sequences for gene-specific qPCR

Gene	Forward Primer (5'-3')	Reverse Primer (5'-3')
GAPDH	GGAGCGAGATCCCTCCAAAAT	GGCTGTTGTCATACTTCTCATGG
PPIH	TTTGCAGACGTTGTGCCTAAG	CCTTTGTATCCTATTGGAACCCC
CyclinA1	ACATGGATGAACTAGAGCAGGG	GAGTGTGCCGGTGTCTACTT
CyclinD1	ATCAAGTGTGACCCGGACTG	CTTGGGGTCCATGTTCTGCT
P21	TGTCCGTCAGAACCCATGC	AAAGTCGAAGTTCCATCGCTC
P27	CTGCAACCGACGATTCTTCT	GCATTTGGGGAACCGTCTGA
HNRNPC	GCCAGCAACGTTACCAACAA	TGAACAGAGCAGCCCACAAT
YTHDF1	GCACACAACCTCCATCTTCG	AACTGGTTCGCCCTCATTGT
YTHDF2	AGCCTCTTGGAGCAGTACAAAA	TTATTGGGCCTTGCCTGTGG
RBM15	GGAAGTCGAGTCCTCACCAC	ACGACCCGCAACAATGAAG
RBM15B	ATTGTGGGAAGGAAAACAGGGT	AACTGTGTAACCACCAGGCA

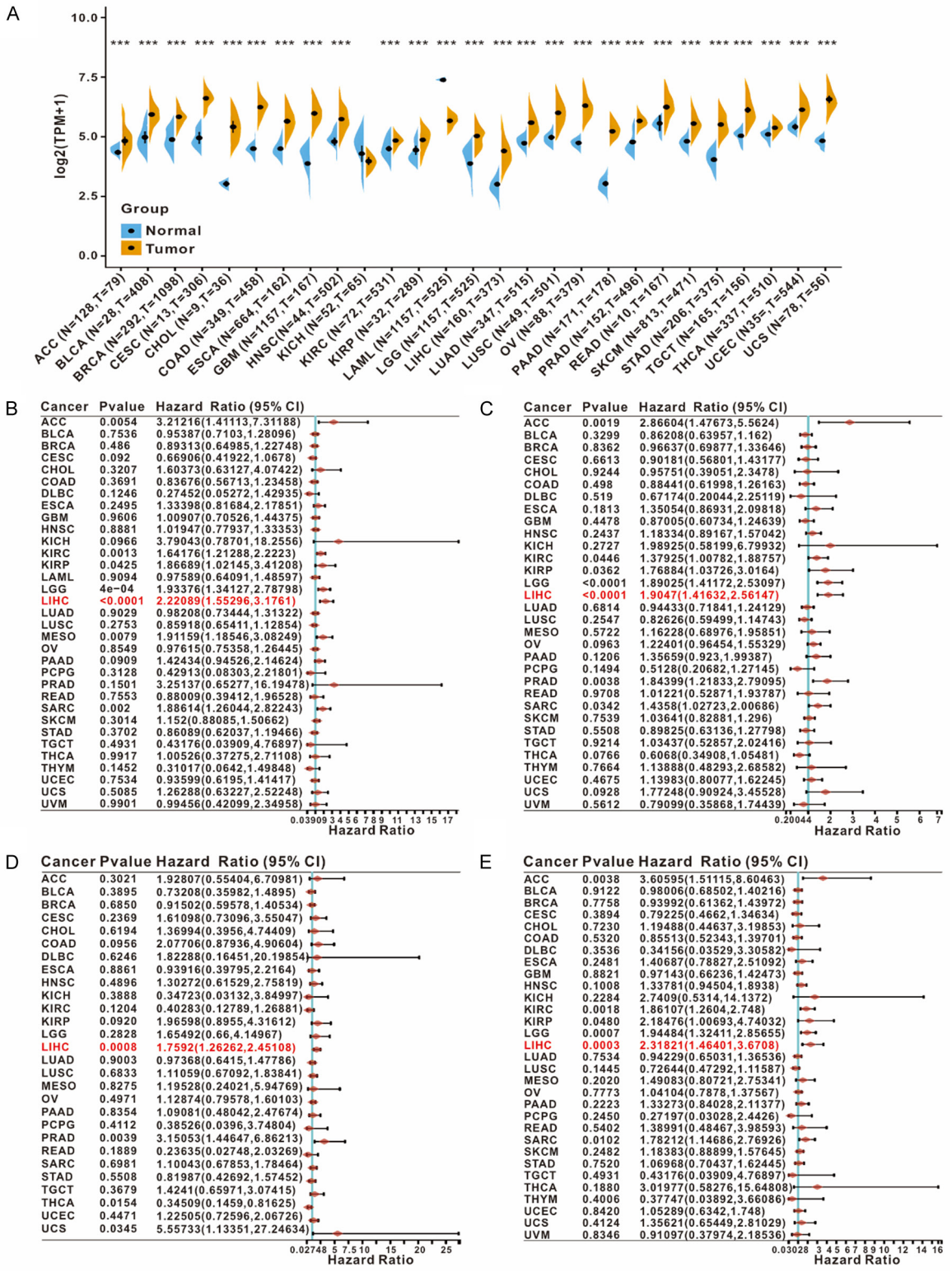

Figure S1. Prognostic value of PPIH across TCGA pan-cancers. (A) Conjoint analysis of TCGA + GTEx data revealed the differential expression of PPIH in tumor tissues compared with normal tissues. The abscissa represents different tumor tissues, whereas the ordinate represents the distribution of PPIH expression. (B-E) Forest plots display the univariate Cox regression analysis of PPIH for OS (B), PFS (C), DFS (D), and DSS (E) across TCGA pan-cancer studies. The hazard ratio is indicated, where HR > 1 suggests PPIH as a risk factor, and HR < 1 indicates a protective factor. OS, overall survival; PFS, progression-free survival; DFS, disease-free survival; DSS, disease-specific survival; ***P < 0.001.

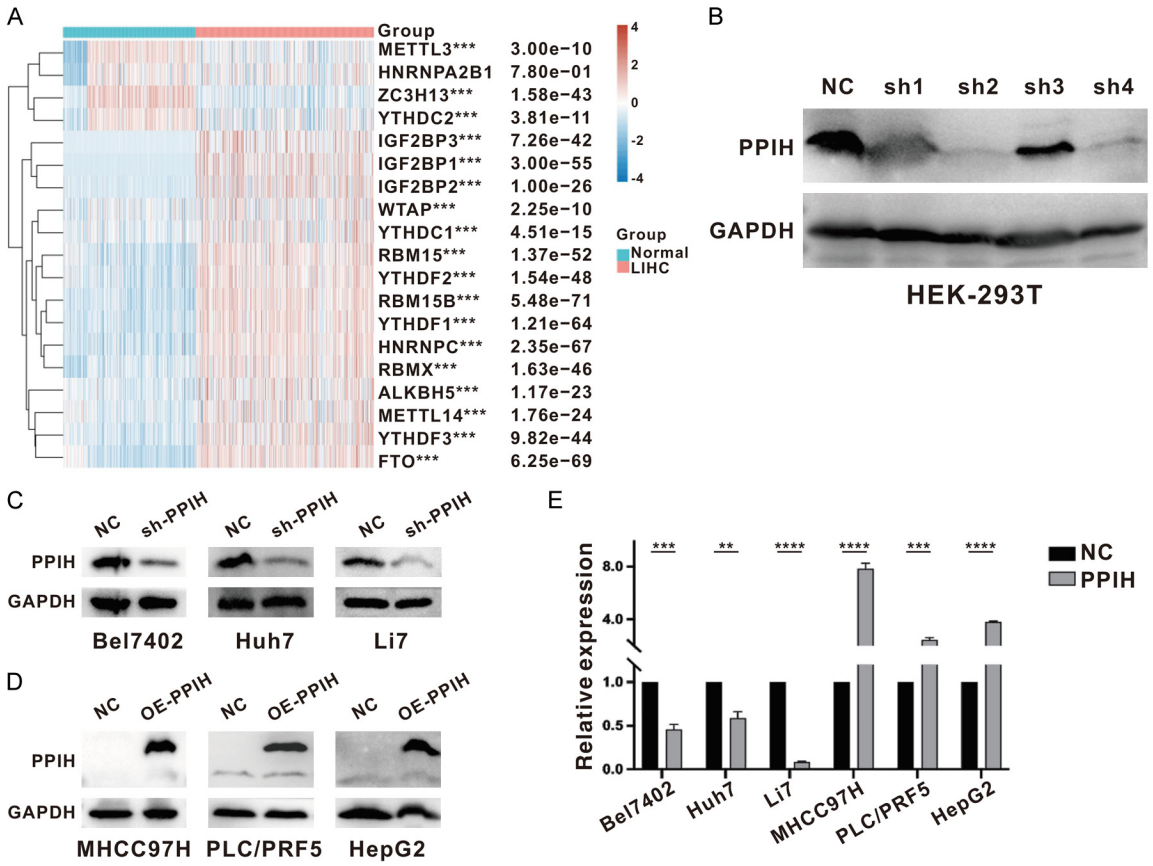

Figure S2. m6A methylation level and PPIH expression in LIHC. A. Expression profiles of m6A modification-related genes in normal tissues (n = 276) and LIHC tissues (n = 371). B. Western blot analysis was used to assess the PPIH knockdown efficiency in HEK293T. C. Western blot analysis was used to verify the PPIH knockdown efficiency in Bel7402, Huh7, and Li7 cells at the protein level. D. Western blot analysis was used to verify the PPIH overexpression efficiency in MHCC97H, PLC/PRF/5, and HepG2 cells at the protein level. E. qPCR was used to verify the knockdown and overexpression efficiency at the transcription level. qPCR, quantitative polymerase chain reaction; LIHC, liver hepatocellular carcinoma; **P < 0.01, ***P < 0.001, ****P < 0.0001.